Quantifying the impact of chronic lead toxicity on the American Bald Eagle *(Haliaeetus leucocephalus)* population in the Great Lakes Region

Christine Brašić[1], Latimer Harris-Ward[2], Fabio A. Milner[3], Carlos Bustamante-Orellana[3], Jordy Cevallos-Chavez[3] and Leon Arriola[1]

[1] *University of Wisconsin-Whitewater*
[2] *University of the Pacific*
[3] *Arizona State University*

December 30, 2020

Abstract

The bald eagle, an American Icon, was recognized as an endangered species in 1967 after its population dropped to critically low numbers due to the adverse reproductive effects of DDT. After DDT was banned in 1972, another environmental contaminant continued to affect their recovery, lead. Ingestion of lead-based ammunition was shown to be the eagles' top cause of death, resulting in a 1991 ban of its use for waterfowl hunting. Nearly thirty years later, lead-toxicity in bald eagles persists. The main source of lead is now carrion contaminated with lead from hunters' ammunition. Lead-toxicity may have severe clinical consequences (including death), but also more subtle, chronic ones such as reduced fertility and voracity. We formulate an ODE model to describe the progression through different stages of lead-toxicity and its impact on the dynamics of the eagle population. We compare and contrast the impact of percentage of contaminated carrion vs. treatment of lead-toxicity. Our results suggest that the health of bald eagle population in the Great Lakes region is more sensitive to the percentage of available contaminated carrion than to the treatment of lead-toxicity.

1 Introduction

The American bald eagle, *Haliaeetus leucocephalus*—an apex predator, plays an important ecological role in the Laurentian Great Lakes region of the Midwestern United States. However, the presence of spent lead ammunition in the environment causes lead poisoning in bald eagles, which has adverse ecological effects influencing many components of the ecosystem. Being an apex predator, the bald eagle establishes ecological stability within the Great Lakes ecosystem. Studies show that the absence of apex predators causes trophic cascades, leading to ecological degradation, and increases the populations of mesopredators [8, 33]. This would further degrade the mesopredator-prey dynamics resulting in over-hunting and possible extinction of the prey [33]. Other ecological effects include an increase in competition between prey leading to additional extinctions [7]. Moreover, studies of contamination in predatory bird populations are often used to evaluate the general contamination of their environment [27].

The Great Lakes region has significant environmental, ecological and economic importance. The Great Lakes make up 18%-21% of the world's freshwater used for drinking and are essential for commercial and recreational fisheries that, accounting for secondary services like lodging, restaurants and marinas, account for over $19 billion dollars in annual sales and $6.4 billion dollars in revenue for over 250,000 jobs [1, 25, 40]. About 7% of American farm production originates in the Great Lakes region, with a population of over 30 million—roughly 9% of the U.S. population [1].

The Bald Eagle first gained federal protection in 1940, when Congress passed the Bald Eagle Protection Act. Later, the Protection Act was amended to also include the Golden Eagle [52]. Lead poisoning in eagles is indirectly caused by the use of leaded ammunition in large game hunting. Many studies show that lead toxicity has been one of the main threats to Bald Eagle populations. For instance, some studies show that feasting on killed deer constitutes a major source of lead exposure to scavenging birds in the wild such as Bald Eagles [31, 36, 50].

Acute and chronic effects of lead toxicity on the bald eagles have been the focus of a recent study [3]. Being large birds of prey with opportunistic foraging habits, eagles are easy victims of ingestion of toxic substances from poisoned or shot carcasses. Data on causes of mortality for 552 Bald and Golden Eagles examined at the National Wildlife Health Center (NWHC) in Madison, Wisconsin, from 1975 through 2013, were published by Russell and Franson [39]. However, it is difficult to quantify the chronic effects of lead toxicity in bald eagles because their natural depuration rate of lead is 3 weeks [2]. Despite the many articles that explore chronic lead toxicity, e.g. [13, 18] and acute effects [16, 45] of lead toxicity, there do not seem to be any that propose mathematical models to study the dynamics of the bald eagle population based on lead toxicity levels. This motivates our research: using a system of ordinary differential equations based on a compartmental model, we successfully quantify the impact of chronic lead toxicity on the American Bald Eagle population in the Great Lakes region.

Through numerical simulations, we forecast the 25-year size of the bald eagle population (at the current rates of winter food-source contamination) to reach approximately 35,200. When we remove the source of contamination to simulate the population dynamics in the

absence of lead, we observe that there is a 1.2% increase in their number (from 35,208 to 35,638). Also, varying the per capita rate at which eagles are retrieved and given chelation therapy and rehabilitation, we find that the number of eagles increases by a mere 0.07% (35,221 up from 35,197 bald eagles). Through the use of sensitivity analysis, we were able to identify that the removal of lead from the environment has a much greater positive effect on the bald eagle population than treating and rehabilitating eagles with chronic lead toxicity.

2 Methodology

2.1 Location of Studied Population and Data Used

We consider the eight states that surround the Great Lakes of the United States: Illinois, Iowa, Indiana, Michigan, Minnesota, Missouri, Ohio, and Wisconsin. North central Wisconsin has one of the highest densities of occupied bald eagle nesting territories in North America [28]. Although the bulk of the bald eagle population is contained in the northern states, eagles do migrate and spend winters in the states to the south [43]. We find it reasonable to include states to the south of the Great Lakes because there exists a correlation between lead-toxicity levels and lead accumulation during the winter [26, 31, 39, 44]. After defining our region, we composed a set of occupied bald eagle nests obtained from the United States Fish and Wildlife Service (USF&WS) data, the relevant Departments of Natural Resources (DNRs), and the Center for Biological Diversity [10,28,35,41,48]. Occupied nests are defined as those in which an incubating adult, eggs, young, or nest repair is observed [28]. We report our results using total bald eagle population values for the region. According to the USF&WS [48], bald eagles over the age of four constitute 43% of the population and incubating adults occupy nests in pairs. This allows us to estimate the total population of eagles through the following calculation:

$$\text{Total Population} = \frac{2}{0.43} * (\text{Number of Occupied Nests}).$$

2.2 Symbolic Manipulations and Numerical Simulations

For symbolic manipulations, both Mathematica Version 12.1 [23] and Maple (2019) [30] were used. For numerical simulations we utilized MATLAB R2019a and R2020a [22] and R version 3.6.1. The data was prepared using the same version of R.

2.3 Assumptions

In order to model the effects of lead-toxicity on the population of bald eagles, we assume lead as the only anthropogenic factor affecting the population. Bald eagles exhibit seasonal scavenging behavior aligned with the big-game hunting seasons [5,31,50]. Many studies suggests a strong correlation between lead-based ammunition, hunting seasons, and lead-toxicity in scavenging species [4, 6, 14, 15, 17–19, 36]. Since the 1991 ban of lead-based ammunition for waterfowl hunting, lead-shot-contaminated carrion from unretrieved deer is now thought to be the bald eagle's main source of exposure to lead [39, 45]. Hence, we shall assume that

eagles acquire lead-toxicity through the consumption of lead-contaminated carrion. Carrion is assumed to be uniformly distributed in the ecosystem during the annual fall and winter hunting season at a constant rate [38,50]. Likewise, we shall assume a uniform concentration of lead in each kilogram of contaminated carrion. Since the population of eagles are also assumed to be uniformly distributed throughout the region, they have an equal probability of consuming contaminated carrion.

We model lead-toxicity by dividing the population into four disjoint compartments, corresponding to the populations of lead-free eagles, those with one of two-stages of lead-toxicity and those under treatment for lead-toxicity. Additionally, we assume that the time eagles spend in each compartment is exponentially distributed and the stages of lead-toxicity are determined by the serum lead levels: eagles with serum lead levels under 0.2 ppm are considered lead-free, as these levels are considered background [17]; eagles with serum lead levels between 0.2 and 0.5 ppm are classified as having Sub Clinical lead (Pb) Toxicity (SCPT) [17]; eagles with serum lead levels over 0.5 ppm are classified as having Clinical lead (Pb) Toxicity (CPT) [17]. We model the subtle, long-term damage of SCPT eagles through a reduction in fertility and voracity [18,38]. Due to the severity of CPT [37,39], we assume eagles with CPT either succumb to lead-poisoning or are retrieved and given therapy and rehabilitation. Hence, we shall assume that all non-natural mortality of eagles is due to CPT or failure of CPT treatment. Eagles with CPT do not reproduce and, since CPT is the final stage of lead-toxicity, we may assume that they do not continue to accumulate lead from further consumption of contaminated carrion. If treatment of CPT is successful, these eagles retain lasting physiological damage [9] and, therefore, we return them to the SCPT compartment in our model rather than to that of lead-free eagles.

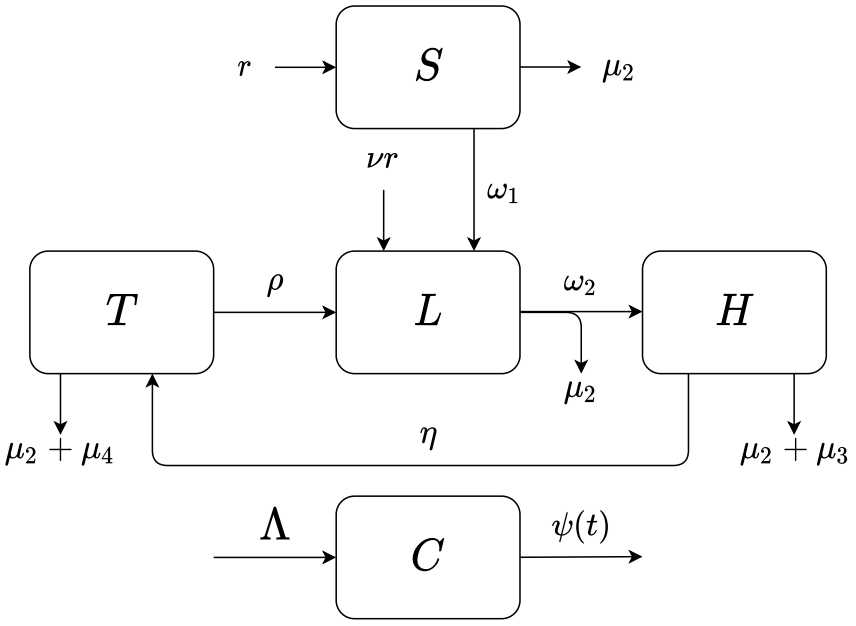

Figure 1: Schematic flow diagram for our mathematical model. The model consists of five compartments: lead-free Eagles (S), SCPT eagles (L), CPT eagles (H), and eagles in treatment (T), and a compartment for contaminated carrion (C).

Lead readily binds to calcium, settling in the bones of eagles over time [18]. Lead accumulated within the bones remains stable for long periods of time, but during egg-formation may re-mobilize into the bloodstream, accumulating in eggshells and thus allowing the vertical transmission of lead-toxicity to the newborn eaglets [3,4,13,15,49]. For these reasons, we assume eagles with SCPT only beget eagles with SCPT and lead-free eagles beget lead-free eagles. Lastly, we assume a closed ecosystem, i.e. the eagle population is not affected by migration. We assume the population grows logistically in the absence of lead.

2.4 Model Formulation

1. **Contaminated carrion: $\mathbf{C = C(t)}$**

   We shall assume that contaminated carrion is the only source of lead for the bald eagle population and that it increases at a constant annual rate, Λ, representing the annual mass of unretrieved game containing fragments of spent lead-ammunition. Bald eagles periodically scavenge and are hence exposed to lead toxicity by consuming the contaminated carrion [31, 50]. Eagles may also scavenge uncontaminated carrion, so we consider the percentage of carrion that is contaminated by dividing C by the total annual input of carrion, M. Both lead-free and SCPT eagles feast on carrion, at their respective per capita rates (δ_1 and δ_2), reducing the amount in the environment. Carrion also decreases by natural decomposition (at unit rate μ_1). These assumptions lead to the following ODE describing the dynamics of C:

$$\frac{dC}{dt} = \Lambda - \delta_1 \frac{C}{M} S - \delta_2 \frac{C}{M} L - \mu_1 C. \tag{1}$$

2. **Lead-free eagles: $\mathbf{S = S(t)}$**

   Lead-free (or uncontaminated) eagles increase in number via their natural per capita birth rate, r. Since these eagles have little to no lead contamination, they reproduce with unaffected fertility. We assume that their growth rate is logistic when taking into account the entire eagle population $S+L+H+T$, with a carrying capacity K for the Great Lakes region. As uncontaminated eagles scavenge contaminated carrion, they become victims of lead toxicity [6]. They move to the SCPT compartment (L) at a per capita rate ω_1 when all available carrion is contaminated with lead. Lead-free eagles are assumed to be healthy, so they die a natural death (at per capita rate μ_2), not due to lead toxicity.

$$\frac{dS}{dt} = rS\left(1 - \frac{S+L+H+T}{K}\right) - \omega_1 \frac{C}{M} S - \mu_2 S. \tag{2}$$

3. **Eagles with sub-clinical lead toxicity: $\mathbf{L = L(t)}$**

   SCPT eagles have been exposed to lead; their blood contains detectable levels of lead in the range of 0.2 to 0.5 ppm but they do not exhibit clinical symptoms [17]. Although SCPT eagles have no readily observable symptoms of lead-toxicity, they do suffer physiological damage from chronic, sub-clinical serum lead-levels leading to reduced appetite

(per capita scavenging rate $\delta_2 = w\delta_1, 0 < w < 1$) and reduced per capita fertility rate ($vr, 0 < v < 1$) [18, 38]. SCPT eagles also exhibit logistic growth, but they contribute less to the population of eagles, due to the their damaged fertility. Their offspring are born into the SCPT class due to vertical (maternal) transmission of lead to newborn eaglets [3, 4, 15, 49]. Inflow to the SCPT class comes both from lead-free eagles, at a per capita rate ω_1, and from eagles leaving treatment, at a per capita rate ρ. Eagles leaving treatment suffer lasting damage and chelation therapy does not reduce their serum lead levels down to zero; hence they return to the SCPT class rather than to the lead-free [9]. The per capita outflow rate from the SCPT, ω_2, is less than the per capita inflow rate into this compartment, ω_1 because of two reasons. First, SCPT eagles have a reduction in appetite; second, the amount of lead that must be accumulated to move each one of them into the CPT compartment is larger than the amount of lead needed to move a lead-free eagle into the SCPT compartment. SCPT eagles suffer chronic physiological damage, but do not succumb to death via lead toxicity in this compartment, therefore, we shall assume that they only die from natural causes, at per capita rate μ_2.

$$\frac{dL}{dt} = vrL\left(1 - \frac{S + L + H + T}{K}\right) + \omega_1 \frac{C}{M} S + \rho T - \omega_2 \frac{C}{M} L - \mu_2 L \tag{3}$$

4. **Eagles with clinical lead toxicity: $\mathbf{H} = \mathbf{H}(\mathbf{t})$**

CPT eagles have serum lead-levels high enough (> 0.5 ppm) to exhibit observable signs of lead-toxicity (e.g. difficulty flying, gross lesions on organs, total loss of appetite, etc) [9, 18]. SCPT eagles flow into the clinical compartment at a per capita rate ω_2 when all available carrion is contaminated with lead (proportionally reduced by the percentage of lead-contaminated carrion among all available carrion). CPT eagles may succumb to death via lead-toxicity (at per capita rate μ_3), through natural death (at per capita rate μ_2), or they may be retrieved for veterinary care, at a per capita rate η. This retrieval rate moves them to the treatment compartment. Eagles with clinical lead-toxicity are not healthy enough for reproduction. Since we assume eagles at this stage of lead-toxicity either succumb to poisoning or are rescued, they do not interact with contaminated carrion and do not increase their lead levels.

$$\frac{dH}{dt} = \omega_2 \frac{C}{M} L - (\eta + \mu_2 + \mu_3) H, \tag{4}$$

5. **Eagles in treatment: $\mathbf{T} = \mathbf{T}(\mathbf{t})$**

The treatment compartment comprises eagles under veterinary intervention and rehabilitation when exhibiting clinical symptoms of lead-toxicity. CPT eagles flow into the treatment compartment at the per capita rate η at which humans find, capture and treat lead-poisoned eagles. Since chelation therapy carries its own risks [9, 37], it is administered until eagles reach sub-clinical rather than background levels of lead so that,

when released, these eagles are not considered lead-free. Lead-toxicity causes lifelong physiological damage [36], therefore we assume after rehabilitation, they reach sub-clinical biological capacity. Eagles in treatment may die a natural death (at per capita rate μ_2) and they may also be euthanized (at per capita rate μ_4). If the eagles survive the treatment and are declared fit, they may be released to join the wild eagle population (at per capita successful treatment rate ρ) [37].

$$\frac{dT}{dt} = \eta H - (\rho + \mu_2 + \mu_4)T, \tag{5}$$

Combining some parameters, our model can be described by the following non-linear system of ordinary differential equations:

$$\frac{dC}{dt} = \Lambda - \tau_1 CS - \tau_2 CL - \mu_1 C, \tag{6}$$

$$\frac{dS}{dt} = rS\left(1 - \frac{S+L+H+T}{K}\right) - \omega_1 CS - \mu_2 S, \tag{7}$$

$$\frac{dL}{dt} = vrL\left(1 - \frac{S+L+H+T}{K}\right) + \omega_1 CS + \rho T - \omega_2 CL - \mu_2 L, \tag{8}$$

$$\frac{dH}{dt} = \omega_2 CL - \xi_1 H, \tag{9}$$

$$\frac{dT}{dt} = \eta H - \xi_2 T, \tag{10}$$

where,

$$\tau_1 = \frac{\delta_1}{M}, \quad \tau_2 = \frac{\delta_2}{M}, \quad \xi_1 = \eta + \sigma_1, \quad \sigma_1 = \mu_2 + \mu_3, \quad \xi_2 = \rho + \sigma_2 \text{ and } \sigma_2 = \mu_2 + \mu_4.$$

The parameters τ_1 and τ_2 represent, respectively, the *unit per capita consumption rates* of contaminated carrion by lead-free and by SCPT eagles. The total eagle population, N, at time t is given by:

$$N(t) = S(t) + L(t) + H(t) + T(t) \tag{11}$$

2.5 State Variables Definitions and Parameter Calculations

Eagles consume lead through scavenging lead-shot-contaminated carrion. We shall assume that this is their only source of lead. Contaminated carrion enters the ecosystem during the annual fall and winter deer-hunting firearm season [53]. Using 2012, 2013, and 2019 deer harvest reports from the region of study [34, 50, 51], along with a 2009 study from Iowa, we estimate an annual harvest rate of 900,000 deer. Studies suggest between 10% and 32% of deer that are shot are not retrieved by hunters [31, 32, 50]. Since the data does not account for poaching, discarded offal, and other unreported additions to the overall annual deposit of carrion, we assume that 32% of hunted deer go unretrieved, giving 280,000 deer per year. Taking the average mass of a deer in Wisconsin to be 72 kilograms [51], we compute the

total annual mass of carrion, M—an estimated 20 million kilograms. To obtain the proportion of lead-contaminated carrion, we use a 2008 study from the US Department of Health and Human Services which found 15% of venison donated to Wisconsin food pantries to be contaminated with lead [12]. Assuming the proportion of lead-contaminated venison in food pantry donations is the same as that for unretrieved deer, we estimate the input rate of contaminated carrion, Λ, as 3 million kilograms per year.

A 2009 study of scavengers and animal decomposition in Wisconsin found that a deer carcass will remain in the environment for 18 to 55 days during the fall and winter seasons [24]. Adjusting this value to an annual rate, we estimate the natural unit decay rate of carrion, $\mu_1 = 1$ year^{-1}. To obtain the consumption rates of carrion by bald eagles, we use estimates provided by The American Eagle Foundation. They state a bald eagle averages an annual consumption rate between 219 and 365 pounds [5]. Taking the average of those rates and converting the result to kilograms, we estimate the per capita consumption rate for lead-free eagles, δ_1, as 132 kg/yr. We model the physiological effect of chronic lead-toxicity through a reduction in voracity and fertility. Although several studies note a reduction in voracity as a physiological effect of lead-toxicity [11,17,18], quantification of affected voracity at different stages of lead-toxicity is not available. We assume a conservative proportion of retained voracity, $w = 0.9$. Multiplying this hypothesized proportion of retained voracity by the per capita consumption rate of lead-free eagles, we estimate the per capita consumption rate of eagles with SCPT, δ_2, as 118.8 Kilograms per year.

Consumption of contaminated carrion serves as a proxy by which eagles accumulate lead, allowing them to traverse the stages of lead-toxicity. The per capita rate for lead-free eagles to acquire SCPT when all carrion is contaminated, ω_1, is estimated using the annual percent change of lead-free, SCPT, and CPT bald eagles submitted to Iowa wildlife rehabilitation facilities between the years 2007 and 2008 [31]. The average annual change in the number of eagles with SCPT is estimated to be 9.5%. Converting this value to annual rate of change, we obtain an estimate for the per capita rate at which a lead-free eagles acquire SCPT when all carrion is contaminated, $\omega_1 = 0.100$ per year. Similarly, the per capita rate at which eagles with SCPT acquire CPT is estimated by first finding the annual *percent* change in the number of CPT eagles and then converting it to the per capita rate at which eagles with SCPT acquire CPT when all carrion is contaminated, $\omega_2 = 0.142$ per year.

In the absence of lead, we assume the bald eagle population grows logistically. A clearly defined carrying capacity for the bald eagle population in the Great Lakes region does not exist. In 2016, the US Fish and Wildlife Service determined the carrying capacity of the bald eagle, for the entire United States, as $227,800$ [48]. The study concludes an expectation for the growth rate of the population to remain consistent with the growth rate in 2009. For 2009, according to data contained in that study, the Great Lakes Region contained approximately 20% of the country's bald eagle population. Assuming that the average growth rate for the entire country is maintained, then the proportion of eagles in the Great Lakes region is maintained as well and we may set the carrying capacity for the bald eagle in the Great Lakes region as 20% of that for the US, that is $K \approx 46,000$. This study also calculates the annual growth rate in the absence of anthropogenic factors as 0.206. Since we assume lead-toxicity as the only anthropogenic factor affecting bald eagles, we use the USF&WS value for the bald eagle population's growth rate, r. Chronic lead-toxicity is shown to damage reproductive organs [9, 37] but the reduction in fertility has not been quantified. Using a

2017 study regarding lead-toxicity-induced fertility reduction of Bonelli eagles [15], we make a conservative estimate for the proportion of retained fertility by SCPT eagles, $v = 0.7$. To model affected fertility of eagles with SCPT, we multiply this value by the natural growth rate to obtain the growth rate of the SCPT eagles.

Eagles with CPT have considerable long-term physiological damage, including gross ocular, neurological, and cardiac lesions [9], along with a weakened bone structure [13]. Due to intraspecific competition for mating [47], we assume that bald eagles with CPT are not capable of reproduction. Upon reaching the final stage of lead-toxicity, CPT, eagles die a natural death, die due to lead-poisoning, or are retrieved and provided veterinary care—chelation therapy and rehabilitation [9, 29, 31, 37]. Since it is entirely dependent on human intervention, the per capita treatment rate of eagles with CPT, η, functions as a control parameter in the model. We vary this parameter in our simulations, but set our initial value assuming that the probability for an eagle with CPT to be found and placed into treatment is 69.3%, that results in a per capita rate $\eta = 0.5$. The majority of eagles with CPT are treated during the hunting season [3, 29, 50]. Since bald eagles begin courtship and nest construction during the winter [42, 43, 50], we assume CPT eagles that are in treatment during the mating season do not reproduce. Chelation therapy and rehabilitation takes anywhere from weeks to months [9, 37, 38]. Hence, the per capita recovery rate from therapy, ρ, is set to 4 per year, representing an average duration of treatment of 13 weeks. Over the course of a year, approximately 20% of eagles in treatment are euthanized [46, 54]. Converting this value to an annual rate, we set the per capita death rate due to treatment failure, $\mu_4 = 0.223$.

We summarize in Tables 1 and 2 all the parameters used in the model, their units, description and values, and the state variables used in our model.

Table 1: **Parameter Definition**

Param.	Description	Units	Values[Reference]
Λ	Contaminated carrion input rate	kg/yr	3,000,000 [12]
δ_1	Per capita consumption rate of lead-free eagles	kg/yr	132 [5]
δ_2	Per capita consumption rate of eagles with SCPT	kg/yr	118.8 [5]
M	Constant total mass of carrion available for consumption	kg	2×10^7 [34, 50, 51]
μ_1	Natural unit decay rate of carrion	$1/yr$	1 [24]
μ_2	Natural per capita death rate of eagles	$1/yr$	1/30 [5]
μ_3	Lead-induced per capita death rate of eagles	$1/yr$	365/133 [17]
μ_4	Per capita death rate of eagles due to treatment failure	$1/yr$	0.223 [46]
ω_1	Per capita rate to become SCPT when $C = M$	$1/yr$	0.142 [31]
ω_2	Per capita rate to become CPT when $C = M$	$1/yr$	0.100 [31]
r	Bald Eagle per capita birth rate	$1/yr$	0.206 [48]
K	Carrying capacity for bald eagles in Great Lakes region	1	46,000 [48]
v	Proportion of retained fertility by SCPT eagles	1	0.7 [15]
w	Proportion of retained voracity by SCPT eagles	1	0.9 [Estimated]
ρ	Per capita recovery rate from therapy	$1/yr$	4 [9, 37, 38]
η	Per capita treatment rate of CPT eagles	$1/yr$	0.5 [Variable, 0-1]

Table 2: **Variable Definition**

Variable	Description	Units
C	Mass of contaminated carrion	kg
S	Population of lead-free eagles	Non-dimensional
L	Number of eagles with SCPT	Non-dimensional
H	Number of eagles with CPT	Non-dimensional
T	Number of eagles in treatment	Non-dimensional

3 Analysis

We include here some mathematical results that have two goals: first, show that the model is biologically meaningful in the sense that, from non-negative initial conditions, it produces non-negative solutions for all time; moreover, if the initial conditions place the total population size below the carrying capacity, then it stays below the carrying capacity for all time. Secondly, we provide some analysis of the local stability of equilibrium points because it is related to the long-term behavior of solutions that can provide ecologically relevant insights into the impact of various types of interventions.

3.1 Positivity of Solutions

We need to prove that the system (6)-(10) supplemented with non-negative initial conditions, has non-negative global solutions. We shall assume that $S(0) > 0$. Moreover, we shall assume that $\Lambda = \Lambda(t)$ is a positive constant on the intervals $[n, n + 0.25]$ and it vanishes on the intervals $(n + 0.25, n + 1)$, for all $n \in \mathbb{Z}$. This choice of Λ is motivated because contaminated carrion is only produced during the hunting season that lasts three months. Under these two conditions we can prove the stronger result that, with non-negative initial conditions, all state variables are strictly positive for all positive times.

First note that the general existence and uniqueness theorem for systems of ODEs ensures that a unique solution exists for $t \in [0, +\infty)$. Next note that (6) guarantees that C is strictly positive for $0 < t < +\infty$): in fact, with $g(t) = \tau_1 S(t) + \tau_2 L(t) + \mu_1$ and $G(t) = \int_0^t g(s)ds$, we have

$$C(t) = C(0)e^{-G(t)} + \Lambda \int_0^t e^{G(s)-G(t)} ds > 0,$$

on the intervals $[n, n + 0.25]$ $(n \in \mathbb{Z})$ because $\Lambda(n) > 0$; therefore, it is also strictly positive on the intervals $(n + 0.25, n + 1)$ $(n \in \mathbb{Z})$ because $C(n + 0.25) > 0$ for all $n \in \mathbb{Z}$. Similarly, (7) guarantees that $S(t)$ is strictly positive for $0 < t < +\infty$):

$$S(t) = S(0) \exp\left(\int_0^t \left(r\left(1 - \tfrac{S(\tau)+L(\tau)+H(\tau)+T(\tau)}{K}\right) - \omega_1 C(\tau) - \mu_2 \right) d\tau \right) > 0,$$

because $S(0) > 0$.

Next we would like to prove that

$$L(0), H(0), T(0) \geq 0 \Longrightarrow L(t), H(t), T(t) \geq 0 \text{ for } 0 \leq t \leq \varepsilon,$$

if $\varepsilon > 0$ is sufficiently small. Assume from now on that $C(0), S(0) > 0$. The continuity of all functions involved and $T(0) \geq 0$ imply that the source term $\omega_1 C(t)S(t) + \rho T(t)$ in (8) is strictly positive for $0 \leq t \leq \varepsilon$, if $\varepsilon > 0$ is sufficiently small. Then, the same argument used for C in (6) applies to (8) to prove that $L(t) > 0$ on $(0, \varepsilon]$. Now that C and L are non-negative on the time-interval $[0, \varepsilon]$, we use the same argument on (9) to show that $H(t) > 0$ on $(0, \varepsilon]$. Finally, the same argument works now on (10) to establish that $T(t) > 0$ on $(0, \varepsilon]$. This establishes the local-in-time conservation of positivity. We would like to show now that this is true globally.

Assume that $C(0) > 0$, $S(0) > 0$ —ensuring that $C(t) > 0$, $S(t) > 0$ for $0 \leq t \leq +\infty$— and also, by contradiction, that the solution does not stay non-negative for all time. Let $\bar{t} = \inf\{t > 0 : L(t) = 0 \text{ or } H(t) = 0 \text{ or } T(t) = 0\}$. Note that $L(t), H(t), T(t) > 0$ on the interval $(0, \bar{t})$ and $\bar{t} \geq \varepsilon > 0$.

Note that the source term $\omega_1 C(t)S(t) + \rho T(t)$ in (8) is strictly positive for $0 \leq t \leq \bar{t}$ and, therefore, there exists $\varepsilon_1 > 0$ such that it is also strictly positive for $\bar{t} \leq t \leq \bar{t} + \varepsilon_1$. Hence, by (8), $L(t) > 0$ on $(0, \bar{t} + \varepsilon_1]$ if $\varepsilon_1 > 0$ is sufficiently small.

We now have the source term in (9), $\omega_2 CL$, is strictly positive on $(0, \bar{t} + \varepsilon_1]$. Hence, by (9), we deduce that $H(t) > 0$ on $(0, \bar{t} + \varepsilon_1]$.

Finally, given that now the source term ηH in (10) is strictly positive on $(0, \bar{t} + \varepsilon_1]$, it follows from (10) that $T(t) > 0$ on $(0, \bar{t} + \varepsilon_1]$.

We have a contradiction because we just found that $L(\bar{t}), H(\bar{t}), T(\bar{t}) > 0$. This proves that $L(t), H(t), T(t) > 0$ for all positive times, if $C(0), S(0) > 0$ and $L(0), H(0), T(0) \geq 0$.

3.2 Boundedness of Total Population by $\left(1 - \frac{\mu_2}{r}\right)K$

Note that summing (7)–(10) we obtain

$$N' = r(S + vL)\left(1 - \frac{N}{K}\right) - \mu_2 N - \mu_3 H - \mu_4 T. \tag{12}$$

We claim that, if $N(0) < \left(1 - \frac{\mu_2}{r}\right)K$, then $N(t) < \left(1 - \frac{\mu_2}{r}\right)K$. for all $t \geq 0$. In fact, if there is $t > 0$ such that $N(t) = \left(1 - \frac{\mu_2}{r}\right)K$, let $\tilde{t}$ be the smallest such time: i.e. $N(\tilde{t}) = \left(1 - \frac{\mu_2}{r}\right)K$ but $N(t) < \left(1 - \frac{\mu_2}{r}\right)K$ for $[0, \tilde{t})$. It then follows from (12) that

$$N'(\tilde{t}) = \mu_2(S(\tilde{t}) + vL(\tilde{t})) - \mu_2\left(1 - \frac{\mu_2}{r}\right)K - \mu_3 H(\tilde{t}) - \mu_4 T(\tilde{t}) < -\mu_3 H(\tilde{t}) - \mu_4 T(\tilde{t}) < 0,$$

so that, by continuity, $N'(t)$ is negative on some interval $(\tilde{t} - \varepsilon, \tilde{t})$ on which $N(t) < \left(1 - \frac{\mu_2}{r}\right)K$ and, therefore, it is impossible to have $N(t) = \left(1 - \frac{\mu_2}{r}\right)K$ for any $t > 0$. The upper bound for the total population size,

$$N_{\text{sup}} = \left(1 - \frac{\mu_2}{r}\right)K,$$

is the *effective carrying capacity* rather than K itself, because we have chosen to represent by r just the per capita birth rate rather than the difference between the per capita birth and death rates.

3.3 Steady States of the System

The equilibrium points of system (1)-(5) are the zeros of the following system of linear and quadratic equations,

$$\Lambda - \tau_1 CS - \tau_2 CL - \mu_1 C = 0, \tag{13}$$
$$rS\left(1 - \tfrac{S+L+H+T}{K}\right) - \omega_1 CS - \mu_2 S = 0, \tag{14}$$
$$vrL\left(1 - \tfrac{S+L+H+T}{K}\right) + \omega_1 CS + \rho T - \omega_2 CL - \mu_2 L = 0, \tag{15}$$
$$\omega_2 CL - \xi_1 H = 0, \tag{16}$$
$$\eta H - \xi_2 T = 0. \tag{17}$$

In the rest of the paper we use asterisks next to the symbol representing state variables to denote their steady states. Solving equation (13) for C, we obtain

$$C^* = \frac{\Lambda}{\tau_1 S^* + \tau_2 L^* + \mu_1} \tag{18}$$

and, solving equation (14) for S, results in the following two alternatives:

$$S^* = 0 \quad \text{or} \tag{19}$$
$$S^* = \frac{K(r - \omega_1 C^* - \mu_2) - r(H^* + L^* + T^*)}{r}. \tag{20}$$

Then, solving equations (15)-(17) for the three other state variables gives

$$L^* = \frac{\omega_1 C^* S^* + \rho T^*}{\omega_2 C^* + \mu_2 - vr\left(1 - \dfrac{S^* + L^* + H^* + T^*}{K}\right)}, \tag{21}$$
$$H^* = \frac{\omega_2 C^* L^*}{\xi_1}, \tag{22}$$
$$T^* = \frac{\eta H^*}{\xi_2}. \tag{23}$$

We first consider equilibrium points with $L^* = 0$. Substituting this value into equation (22) and the result into equation (23) we obtain $H^* = T^* = 0$ and then equation (15) gives

$$C^* S^* = 0,$$

so that $S^* = 0$ or $C^* = 0$. In the first case, (18) gives $C^* = \frac{\Lambda}{\mu_1} \geq 0$ (if $\Lambda \geq 0, \mu_1 > 0$). Therefore, the first equilibrium point for the system (and the only one with $S^* = L^* = 0$) is

$$\mathbf{x}_1^* = (C^*, S^*, L^*, H^*, T^*) = \left(\frac{\Lambda}{\mu_1}, 0, 0, 0, 0\right),$$

corresponding to the constant level of lead-contaminated carrion balancing the input from hunters' large game killings with their natural decay, and no eagle population.

Next, note that from equation (13), $\Lambda = 0$ if, and only if $C^* = 0$, because we are only considering equilibrium points having all five state variables non-negative. We seek equilibrium points corresponding to this case, $\Lambda = 0$—no input of carrion into the environment—or, equivalently, $C^* = 0$. Equation (16) then yields $H^* = 0$, and hence equation (17) implies $T^* = 0$. Now we are left with just the following reduced system of equations (14)-(15):

$$rS^*\left(1 - \frac{S^* + L^*}{K}\right) - \mu_2 S^* = 0,$$
$$vrL^*\left(1 - \frac{S^* + L^*}{K}\right) - \mu_2 L^* = 0.$$

It is not possible for S^* and L^* to be both nonzero because then we would have $\frac{\mu_2}{r} = \frac{\mu_2}{vr}$, necessitating $v = 1$, which is a contradiction because we know that $v < 1$. Thus, one or both of S^* and L^* must be zero. The latter case, $S^* = L^* = 0$, leads back to the equilibrium $\mathbf{x}_1^*$ but now without carrion too because $\Lambda = 0$. The former case, solving this system of equations, leads to two new equilibrium points, the first one given by

$$\mathbf{x}_2^* = (C^*, S^*, L^*, H^*, T^*) = \left(0, K\left(1 - \frac{\mu_2}{r}\right), 0, 0, 0\right),$$

and the second one given by

$$\mathbf{x}_3^* = (C^*, S^*, L^*, H^*, T^*) = \left(0, 0, K\left(1 - \frac{\mu_2}{vr}\right), 0, 0\right).$$

These cases are represented in the second and third panel of Figure 2, where the population of lead-free eagles (S) and the population of SCPT eagles (L), respectively, grow until they reach their corresponding carrying capacities $K\left(1 - \frac{\mu_2}{r}\right)$ and $K\left(1 - \frac{\mu_2}{vr}\right)$. The equilibrium $\mathbf{x}_3^*$ corresponds to the case where, in the absence of exposure to lead, vertical transmission of lead toxicity makes the compartment L persist. To be biologically meaningful, $\mathbf{x}_2^*$ must be in the non-negative orthant of the 5-dimensional state space, i.e. $S^* > 0$. A necessary and sufficient condition is that the intrinsic per capita growth rate be greater than the natural per capita death rate, that is $r > \mu_2 > 0$. Similarly, $\mathbf{x}_3^*$ is in the non-negative orthant of the 5-dimensional state space if, and only if $L^* > 0$, which is satisfied when $vr > \mu_2$. In reality one would expect that in a lead-free environment, SCPT eagles would be healthier in each new generation so that eventually v would approach 1 and the distinction with the lead-free eagles would disappear. In other words, in an environment that is lead-free any population of eagles at equilibrium will be lead-free.

Lastly, we find the remaining equilibrium points, for which $C^* > 0$ and $L^* > 0$. Solving for C^*, H^*, and T^* in terms of S^* and L^* in (13), (16) and (17), we obtain

$$\begin{aligned} C^* &= \frac{\Lambda}{\tau_1 S^* + \tau_2 L^* + \mu_1}, \\ H^* &= \frac{\omega_2 \Lambda}{\xi_1}\left(\frac{L^*}{\tau_1 S^* + \tau_2 L^* + \mu_1}\right), \\ T^* &= \frac{\eta \omega_2 \Lambda}{\xi_1 \xi_2}\left(\frac{L^*}{\tau_1 S^* + \tau_2 L^* + \mu_1}\right). \end{aligned} \tag{24}$$

We first find the steady-states with $S^* = 0$ (and assume $vr > \mu_2$ to ensure the viability of L) and finally the ones with all state variables positive. Substituting $S = 0$ and the expressions (24) into (15), we obtain the following quadratic for L:

$$c_0 L^2 + c_1 L + c_2 = 0, \tag{25}$$

where

$$\begin{aligned} c_0 &= vr\tau_2\xi_1\xi_2, \\ c_1 &= vr((\mu_1 - \tau_2 K)\xi_1\xi_2 + \omega_2\xi_2\Lambda + \eta\omega_2\Lambda) + \mu_2\tau_2 K\xi_1\xi_2, \\ c_2 &= K\xi_1\xi_2\mu_1\, u_2 + \omega_2\Lambda K(\xi_1\xi_2 - \rho\eta) - vr\mu_1 K\xi_1\xi_2. \end{aligned} \tag{26}$$

If this equation has nonzero real roots, L_1^* and L_2^* (with $L_1^* \geq L_2^*$, say), they lead to two new equilibria:

$$\mathbf{x}_4^* = \left(\frac{\Lambda}{\tau_2 L_1^* + \mu_1}, 0, L_1^*, \frac{\omega_2\Lambda}{\xi_1}\left(\frac{L_1^*}{\tau_2 L_1^* + \mu_1}\right), \frac{\eta\omega_2\Lambda}{\xi_1\xi_2}\left(\frac{L_1^*}{\tau_2 L_1^* + \mu_1}\right)\right),$$

$$\mathbf{x}_5^* = \left(\frac{\Lambda}{\tau_2 L_2^* + \mu_1}, 0, L_2^*, \frac{\omega_2\Lambda}{\xi_1}\left(\frac{L_2^*}{\tau_2 L_2^* + \mu_1}\right), \frac{\eta\omega_2\Lambda}{\xi_1\xi_2}\left(\frac{L_2^*}{\tau_2 L_2^* + \mu_1}\right)\right),$$

both corresponding to the long-term behavior depicted in the fourth panel of Figure 2.

Because $c_0 > 0$, equation (25) has real roots with opposite signs if, and only if $c_2 < 0$. This corresponds to the case of just one additional equilibrium point in the first orthant, $\mathbf{x}_4^*$. The condition $c_2 < 0$ is equivalent to

$$\omega_2\Lambda\left(1 - \frac{\rho\eta}{\xi_2\xi_2}\right) < \mu_1(vr - \mu_2),$$

satisfied if, and only if,

$$\mu_1 > \frac{\omega_2\Lambda\left(1 - \frac{\rho\eta}{\xi_2\xi_2}\right)}{(vr - \mu_2)}, \tag{27}$$

because $\xi_1\xi_2 = (\eta + \sigma_1)(\rho + \sigma_2) > \rho\eta$. The biological interpretation of the constraint (27) is that contaminated carrion needs to decay fast enough to keep SCPT eagles from consuming too much of it and moving into the CPT eagles compartment. The limiting case $c_2 = 0$ makes $L_1^* = 0$ and $\mathbf{x}_4^* = \mathbf{x}_1^*$.

On the other hand, equation (25) has two distinct real positive roots if, and only if $c_2 > 0$, $c_1 < 0$ and $c_1^2 > 4c_0c_2$.

Since we are assuming $vr > \mu_2$, it follows that $c_1 < 0$ is equivalent to the following lower bound for the carrying capacity K:

$$K > \frac{vr(\mu_1\xi_1\xi_2 + \omega_2\xi_2\Lambda + \eta\omega_2\Lambda)}{\tau_2\xi_1\xi_2(vr - \mu_2)}. \tag{28}$$

The condition $c_2 > 0$ (see (27)) is equivalent to

$$\mu_1 < \frac{\omega_2\Lambda\left(1 - \frac{\rho\eta}{\xi_2\xi_2}\right)}{(vr - \mu_2)}. \tag{29}$$

Lastly, the condition $c_1^2 > 4c_0c_2$ is

$$\begin{aligned}\big[vr(\mu_1\tau_2K\xi_1\xi_2+\omega_2\xi_2\Lambda+\eta\omega_2\Lambda)-(vr-\mu_2)\tau_2K\xi_1\xi_2\big]^2\\ >4Kvr\tau_2\xi_1\xi_2\big[\omega_2\Lambda(\xi_1\xi_2-\rho\eta)-\xi_1\xi_2\mu_1(vr-\mu_2)\big],\end{aligned}\tag{30}$$

or, equivalently,

$$\begin{aligned}vr\big(\mu_1\tau_2K\xi_1\xi_2+\omega_2\xi_2\Lambda+\eta\omega_2\Lambda\big)^2+vr\big[(1-\tfrac{\mu_2}{vr})\tau_2K\xi_1\xi_2\big]^2+4K\tau_2\xi_1^2\xi_2^2\mu_1(vr-\mu_2)\\ >2\big(\mu_1\tau_2K\xi_1\xi_2+\omega_2\xi_2\Lambda+\eta\omega_2\Lambda\big)(vr-\mu_2)\tau_2K\xi_1\xi_2\\ +4K\tau_2\xi_1\xi_2\omega_2\Lambda(\xi_1\xi_2-\rho\eta),\end{aligned}\tag{31}$$

Summarizing, if conditions (28) and (29) hold together with (30) or (31), then the two equilibrium points $\mathbf{x}_4^*$ and $\mathbf{x}_5^*$ exist and are distinct in the non-negative orthant of $\mathbb{R}^5$.

To find equilibrium points in the positive orthant of $\mathbb{R}^5$, we substitute equations (24) into (14) to obtain the following relation for the state variables S and L: (we have removed a factor S in the equation because we are interested in equilibria with $S>0$)

$$\begin{aligned}\big[\big((\tau_1S+\tau_2L+\mu_1)(K-L-S)r-K(\mu_2\tau_2L+\mu_2\tau_1S+\Lambda\omega_1+\mu_1\mu_2)\big)\xi_1\\ -\omega_2r\Lambda L\big]\xi_2-\Lambda\eta r\omega_2L=0.\end{aligned}\tag{32}$$

Combining equation (14) multiplied by v with equation (32), we obtain an explicit expression for S^* in terms of L^* at any equilibrium point with $S^*\neq 0$:

$$S^*=\left(\frac{\xi_1\xi_2\tau_2\mu_2(1-v)(L^*)^2+[\xi_1\xi_2((\omega_2-v\omega_1)\Lambda+\mu_1\mu_2(1-v))-\eta\omega_2\rho\Lambda]L^*}{\xi_1\xi_2((1-v)\tau_1\mu_2L^*-\omega_1\Lambda)}\right),\tag{33}$$

Next we substitute equations (24) and (33) into (15) and we obtain the following cubic equation for L^* at any equilibrium point with $S^*, L^*\neq 0$:

$$b_0L^3+b_1L^2+b_2L+b_3=0,\tag{34}$$

where

$$\begin{aligned}b_0&=-\mu_2\,(v-1)\,\xi_2\xi_1r\Big[((((-\xi_1+(-v+1)\,\mu_2)\,\omega_2+\omega_1v\xi_1)\,\xi_2\\ &\quad-\eta\,((v-1)\,\mu_2-\rho)\,\omega_2)\,{\tau_1}^2-(\xi_1\,(-\omega_2+\omega_1\,(v+1))\,\xi_2+\omega_2\eta\,\rho)\,\tau_2\tau_1+\omega_1\xi_1\xi_2{\tau_2}^2\Big],\\ b_1&=(\mu_2((v\omega_1-\omega_2)r-\mu_2(\omega_1-\omega_2))(v-1)K{\tau_1}^2+((-((K\tau_2-v\mu_1-\mu_1)\omega_1+\omega_2\mu_1)(v-1)\mu_2,\\ &\quad+((v-1)\omega_1-\omega_2)\Lambda\,(v\omega_1-\omega_2))r+K\tau_2\omega_1{\mu_2}^2(v-1))\tau_1-(2\,\mu_1(v-1)\mu_2+((v-1)\omega_1\\ &\quad-\omega_2)\Lambda)r\tau_2\omega_1){\xi_2}^2{\xi_1}^2+(2\,\tau_1\omega_1r\Lambda\,\mu_2(v-1)\xi_2+\eta\,(K\rho\,\mu_2(v-1)(r-\mu_2){\tau_1}^2+2((v-1)(\omega_1\Lambda\\ &\quad+\rho\,\mu_1/2)\mu_2+((v-1/2)\omega_1-\omega_2)\Lambda\,\rho)r\tau_1-\tau_2\omega_1r\rho\,\Lambda))\xi_2\omega_2\xi_1+\Lambda\,\eta^2r\rho^2{\omega_2}^2\tau_1,\\ b_2&=(((((((v\omega_1-\omega_2)\tau_1-\tau_2\omega_1)K-((v-1)\omega_1-\omega_2)\mu_1)r+\mu_2K(((v-2)\omega_1\\ &\quad+\omega_2)\tau_1+\tau_2\omega_1))\Lambda-\mu_2\mu_1((K\tau_1+\mu_1)r-K\tau_1\mu_2)(v-1))\xi_1+\omega_1\omega_2r\Lambda^2)\xi_2\\ &\quad+(\Lambda\,r\omega_1+\rho\,((K\tau_1-\mu_1)r-K\tau_1\mu_2))\Lambda\eta\,\omega_2)\xi_2\xi_1\omega_1,\\ b_3&=\Lambda\,(\Lambda\,\omega_1-\mu_1\,(r-\mu_2))\,{\omega_1}^2{\xi_2}^2{\xi_1}^2K.\end{aligned}$$

We thus find equilibrium points with $S^* \neq 0$ given by equation (33) and L^* is a root of equation (34). This could, in principle, lead to three additional equilibrium points. However, our numerical explorations suggest that two roots of this cubic are complex conjugates, so that there is only one real solution L^* that, together with (33), leads to the last equilibrium:

$$\mathbf{x}_6^* = \left(\frac{\Lambda}{\tau_1 S^* + \tau_2 L^* + \mu_1}, S^*, L^*, \frac{\omega_2 \Lambda}{\xi_1} \left(\frac{L^*}{\tau_1 S^* + \tau_2 L^* + \mu_1} \right), \frac{\eta \omega_2 \Lambda}{\xi_1 \xi_2} \left(\frac{L^*}{\tau_1 S^* + \tau_2 L^* + \mu_1} \right) \right).$$

These steady-states $\mathbf{x}_4^*$, $\mathbf{x}_5^*$ and $\mathbf{x}_6^*$, corresponding to the dynamics represented in the fourth and fifth panels of Figure 2, are the only ones with $C^*, L^* > 0$.

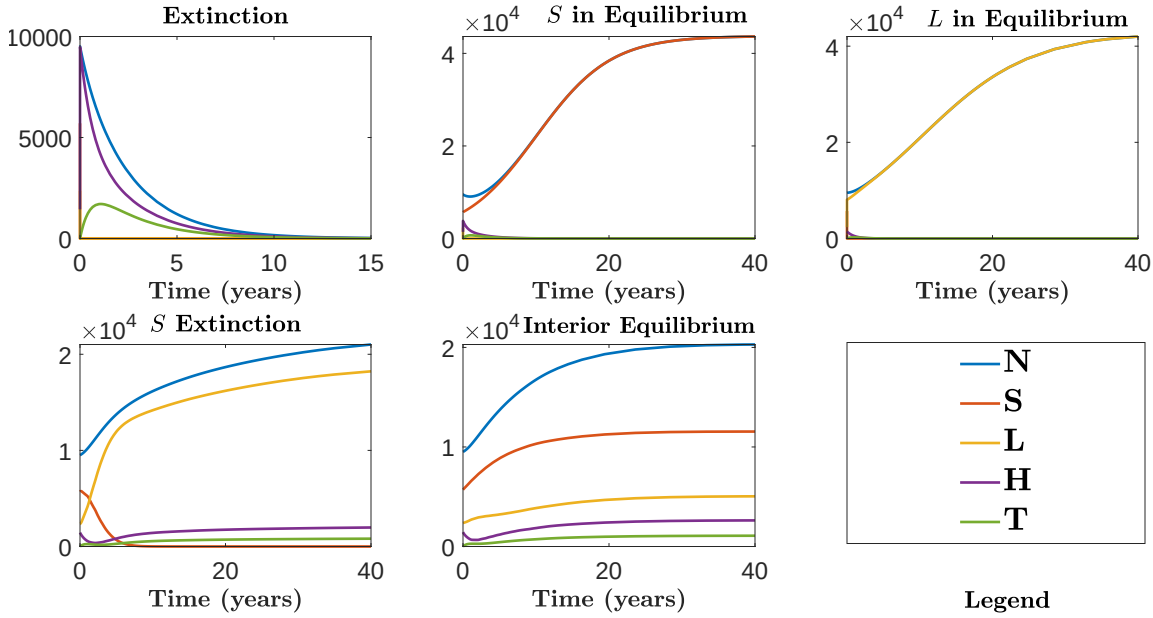

Figure 2: Plots depicting solutions approaching each of the equilibria just described. From left to right and top to bottom, we have $\mathbf{x}_1^*$, $\mathbf{x}_2^*$, $\mathbf{x}_3^*$, $\mathbf{x}_4^*$ and $\mathbf{x}_5^*$ in the fourth panel, and $\mathbf{x}_6^*$.

In order that an equilibrium point be biologically meaningful, it must be in the non-negative orthant of $\mathbb{R}^5$. We have seen that all the coordinates of $\mathbf{x}_4^*$ (respectively, of $\mathbf{x}_5^*$) are positive—except for the second one, $S^* = 0$—if $L_1^* > 0$ (respectively, $L_2^* > 0$), and we also have provided explicit necessary and sufficient conditions for these to hold.

The equilibrium $\mathbf{x}_6^*$ corresponding to the fifth panel in Figure 2 is biologically relevant as long as $S^*, L^* > 0$.

Note: Because of the complex algebraic representation of the coefficients of the cubic equation in L^*, we were unable to provide reasonable algebraic constraints that imply the existence of $\mathbf{x}_6^*$. However, using numerical simulations, we find the model supports its existence.

3.4 Local Stability of Steady States

Determining the stability of the equilibrium points provides useful information about the asymptotic behavior of solutions to our system. First, we compute the Jacobian matrix, given by

$$J = \begin{bmatrix} -L\tau_2 - S\tau_1 - \mu_1 & -\tau_1 C & -\tau_2 C & 0 & 0 \\ -\omega_1 S & \frac{(K-N-S)r - K(\omega_1 C + \mu_2)}{K} & -\frac{rS}{K} & -\frac{rS}{K} & -\frac{rS}{K} \\ -\omega_2 L + \omega_1 S & \frac{\omega_1 KC - rvL}{K} & \frac{v(K-N-L)r - K(\omega_2 C + \mu_2)}{K} & -\frac{rvL}{K} & \frac{-rvL + K\rho}{K} \\ \omega_2 L & 0 & \omega_2 C & -\xi_1 & 0 \\ 0 & 0 & 0 & \eta & -\xi_2 \end{bmatrix}.$$

The Jacobian evaluated at $\mathbf{x}_1^*$ is

$$J(\mathbf{x}_1^*) = \begin{bmatrix} -\mu_1 & -\frac{\tau_1 \Lambda}{\mu_1} & -\frac{\tau_2 \Lambda}{\mu_1} & 0 & 0 \\ 0 & \frac{(r-\mu_2)\mu_1 - \omega_1 \Lambda}{\mu_1} & 0 & 0 & 0 \\ 0 & \frac{\omega_1 \Lambda}{\mu_1} & \frac{(rv-\mu_2)\mu_1 - \omega_2 \Lambda}{\mu_1} & 0 & \rho \\ 0 & 0 & \frac{\omega_2 \Lambda}{\mu_1} & -\xi_1 & 0 \\ 0 & 0 & 0 & \eta & -\xi_2 \end{bmatrix}.$$

The first two diagonal coefficients are eigenvalues, namely

$$\lambda_1 = -\mu_1 < 0$$
$$\lambda_2 = \frac{\mu_1(r-\mu_2) - \omega_1 \Lambda}{\mu_1},$$

negative if, and only if,

$$r - \mu_2 > \frac{\omega_1 \Lambda}{\mu_1}. \tag{35}$$

To find the remaining eigenvalues, we determine roots of the characteristic polynomial of the 3×3 minor obtained by deleting the first two rows and the first two columns, given by

$$p_1(\lambda) = (\lambda + \xi_1)(\lambda + \xi_2)(rv - \lambda - \mu_2)\mu_1 - \omega_2 \Lambda \left(\lambda^2 + (\xi_2 + \xi_1)\lambda + \xi_2 \xi_1 - \eta\rho\right).$$

We utilize Routh's test to determine necessary and sufficient conditions for the stability of x_1^*. Writing $-p_1(\lambda) = a_0\lambda^3 + a_1\lambda^2 + a_2\lambda + a_3$, we obtain the following Routh array

λ^3	a_0	a_2
λ^2	a_1	a_3
λ^1	$(a_1 a_2 - a_0 a_3)/a_1$	
λ^0	a_3	

where

$$
\begin{aligned}
a_0 &= \mu_1, \\
a_1 &= (\mu_2 - rv + \xi_1 + \xi_2)\,\mu_1 + \Lambda\omega_2, \\
a_2 &= \mu_1\xi_1\xi_2 + (\xi_1 + \xi_2)\big[\mu_1(\mu_2 - rv) + \omega_2\Lambda\big], \\
a_3 &= -\xi_1\xi_2\,(-\Lambda\omega_2 + \mu_1\,(rv - \mu_2)) - \Lambda\eta\rho\omega_2.
\end{aligned}
$$

According to Routh's test, we need $a_i > 0,\ i = 0, 1, 2, 3$ and $a_1a_2 > a_0a_3$ to ensure that all the eigenvalues have negative real part. In order to have $a_1 > 0$, we need

$$
rv - \mu_2 < \xi_1 + \xi_2 + \frac{\omega_2\Lambda}{\mu_1}. \tag{36}
$$

For $a_2 > 0$, we need

$$
rv - \mu_2 < \frac{\xi_1\xi_2}{\xi_1 + \xi_2} + \frac{\omega_2\Lambda}{\mu_1},
$$

which follows from (36), because $\xi_1\xi_2 \le 4\xi_1\xi_2 \le (\xi_1 + \xi_2)^2$. In order that $a_3 > 0$, we need

$$
rv - \mu_2 < \left(1 - \frac{\eta\rho}{\xi_1\xi_2}\right)\frac{\omega_2\Lambda}{\mu_1}, \tag{37}
$$

which clearly subsumes (36).

The last condition that needs to be satisfied is $a_1a_2 > a_0a_3$, equivalent to

$$
\begin{aligned}
(\xi_1 + \xi_2)\big(\mu_1^2\xi_1\xi_2 + \mu_1\omega_2\Lambda\big) + \omega_2^2\Lambda^2(1 + \xi_1 + \xi_2) + \mu_1\omega_2\Lambda\rho\eta& \\
> (rv - \mu_2)\mu_1\omega_2\Lambda(1 + \xi_1 + \xi_2),&
\end{aligned} \tag{38}
$$

that is,

$$
rv - \mu_2 < \frac{\omega_2\Lambda}{\mu_1} + \frac{(\xi_1 + \xi_2)\big(\mu_1^2\xi_1\xi_2 + \mu_1\omega_2\Lambda\big) + \mu_1\omega_2\Lambda\rho\eta}{\mu_1\omega_2\Lambda(1 + \xi_1 + \xi_2)}.
$$

This restriction is clearly weaker than (37), which implies that condition (38) holds whenever (37) does.

In summary, the equilibrium point $\mathbf{x}_1^*$ is locally asymptotically stable if

$$
\frac{\omega_1\Lambda}{\mu_1} + \mu_2 < r < \left(1 - \frac{\eta\rho}{\xi_1\xi_2}\right)\frac{\omega_2\Lambda}{v\mu_1} + \frac{\mu_2}{v}
$$

This means that the lead-free eagles per capita birth rate, r, needs to be be in the interval $\left(\frac{\omega_1\Lambda}{\mu_1} + \mu_2, \left(1 - \frac{\eta\rho}{\xi_1\xi_2}\right)\frac{\omega_2\Lambda}{v\mu_1} + \frac{\mu_2}{v}\right)$, that needs to be non-empty. A sufficient condition for this is, for example,

$$
v < 1 - \frac{\eta\rho}{\xi_1\xi_2},
$$

which is $v < 0.8566$ using our parameter values displayed in Table 1. The corresponding range for r in order that $\mathbf{x}_1^*$ be locally asymptotically stable is approximately $(426000, 428571)$, completely outside the realm of nature.

As for $\mathbf{x}_2^*$, the Jacobian is

$$J(\mathbf{x}_2^*) = \begin{bmatrix} \frac{(-K\tau_1-\mu_1)r+K\tau_1\mu_2}{r} & 0 & 0 & 0 & 0 \\ -\frac{\omega_1 K(r-\mu_2)}{r} & -r+\mu_2 & -r+\mu_2 & -r+\mu_2 & -r+\mu_2 \\ \frac{\omega_1 K(r-\mu_2)}{r} & 0 & \mu_2\,(v-1) & 0 & \rho \\ 0 & 0 & 0 & -\xi_1 & 0 \\ 0 & 0 & 0 & \eta & -\xi_2 \end{bmatrix},$$

Its eigenvalues are

$$\begin{aligned} \lambda_1 &= -\xi_2 < 0, \\ \lambda_2 &= -\xi_1 < 0, \\ \lambda_3 &= \mu_2(v-1) < 0, \\ \lambda_4 &= \mu_2 - r < 0, \\ \lambda_5 &= -\frac{\mu_1 + K\tau_1(r-\mu_2)}{r} < 0. \end{aligned}$$

Thus, $\mathbf{x}_2^*$ is locally asymptotically stable. Likewise, for $\mathbf{x}_3^*$, we have

$$J(\mathbf{x}_3^*) = \begin{bmatrix} \frac{-v(K\tau_2+\mu_1)r+K\mu_2\tau_2}{rv} & 0 & 0 & 0 & 0 \\ 0 & -\frac{\mu_2(v-1)}{v} & 0 & 0 & 0 \\ -\frac{\omega_2 K(rv-\mu_2)}{rv} & -rv+\mu_2 & -rv+\mu_2 & -rv+\mu_2 & -rv+\rho+\mu_2 \\ \frac{\omega_2 K(rv-\mu_2)}{rv} & 0 & 0 & -\xi_1 & 0 \\ 0 & 0 & 0 & \eta & -\xi_2 \end{bmatrix},$$

with eigenvalues

$$\begin{aligned} \lambda_1 &= -\xi_2 < 0, \\ \lambda_2 &= -\xi_1 < 0, \\ \lambda_3 &= -\frac{\mu_2(v-1)}{v} > 0, \\ \lambda_4 &= -(rv-\mu_2) < 0, \\ \lambda_5 &= \frac{-K(rv-\mu_2)\tau_2 - rv\mu_1}{rv} < 0. \end{aligned}$$

Because $\lambda_3 > 0$, $\mathbf{x}_3^*$ is an unstable equilibrium.

For the last three equilibria, $\mathbf{x}_4^*$, $\mathbf{x}_5^*$, and $\mathbf{x}_6^*$, determining the asymptotic stability analytically is much more difficult. However, within the range of the parameters of our model, we find that the equilibria $\mathbf{x}_4^*$ and $\mathbf{x}_5^*$ are unstable whereas the equilibrium $\mathbf{x}_6^*$ is locally asymptotically stable.

4 Numerical Simulations

We perform numerical simulations of the evolution of our dynamical system in order to forecast a 25-year evolution of the carrion-bald eagle ecosystem in the Great Lakes region. We also perform them in order to assess the impact of changing the values of parameters for which there are no estimates or those that human intervention can effectively change.

For these simulations, we slightly modify equation (6) and use the following model:

$$\frac{dC}{dt} = \Lambda f(t) - \tau_1 CS - \tau_2 CL - \mu_1 C, \tag{39}$$

$$\frac{dS}{dt} = rS\left(1 - \frac{S+L+H+T}{K}\right) - \omega_1 CS - \mu_2 S, \tag{40}$$

$$\frac{dL}{dt} = vrL\left(1 - \frac{S+L+H+T}{K}\right) + \omega_1 CS + \rho T - \omega_2 CL - \mu_2 L, \tag{41}$$

$$\frac{dH}{dt} = \omega_2 CL - \xi_1 H, \tag{42}$$

$$\frac{dT}{dt} = \eta H - \xi_2 T, \tag{43}$$

where the parameters are the same as in equations (6)-(10) and, for $n \in \mathbb{N}_0$,

$$f(t) = \begin{cases} 1, & n \leq t \leq n + 0.25, \\ 0, & n + 0.25 < t < n + 1. \end{cases}$$

As mentioned earlier, we consider this slightly different model to account for the the fact that input of contaminated carrion, at rate Λ, is seasonal rather than year-round. The factor $f(t)$ acts as a switch. We assume that time $t = 0$ corresponds to the beginning of a hunting season, in November, and that the hunting season lasts for three months.

We begin by showing in Figure 3 how well a logistic curve fits the data for the bald eagle population in the Great Lakes region (we define it as comprising eight states) from 1990 to 2007, thus justifying our population modeling choice to be logistic.

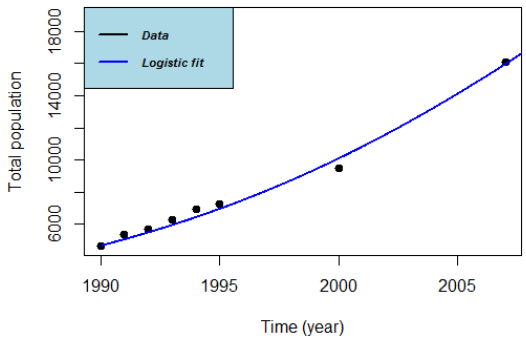

Figure 3: Logistic fit of bald eagle data in Great Lakes region from 1990 to 2007.

The unit decay rate of carrion, μ_1, is not available in the literature. However, there are observations that point to the presence of deer gut piles for 3 weeks to 3.5 months [24] that may suggest a reasonable range of values for μ_1. We examine the impact of varying the parameter μ_1 within the range [0,24], the upper end corresponding to a mean presence of carrion of $\frac{1}{24}$ of a year, or approximately 2.2 weeks.

Figure 4 depicts the changes in the evolution of the system with varying μ_1. The value $\mu_1 = 0$ is used just to show the worst case scenario in which carrion would not decay but only disappear by being entirely consumed by the eagles. It is apparent that the lead-free population is largely unaffected over the 25 years of the simulation. On the other hand, after 25 years, the difference between the number of SCPT eagles when $\mu_1 = 0$ and when $\mu_1 = 24$ is a very significant 1,430 (20%) and, even if we vary the parameter from $\mu_1 = 1$ to $\mu_1 = 24$, the difference in the number of eagles with SCPT is still a significant 830 (12%). This is quite useful information, albeit difficult to act upon because increasing the value of μ_1 through human intervention entails the physical removal of lead-contaminated carrion from the eagles' environment.

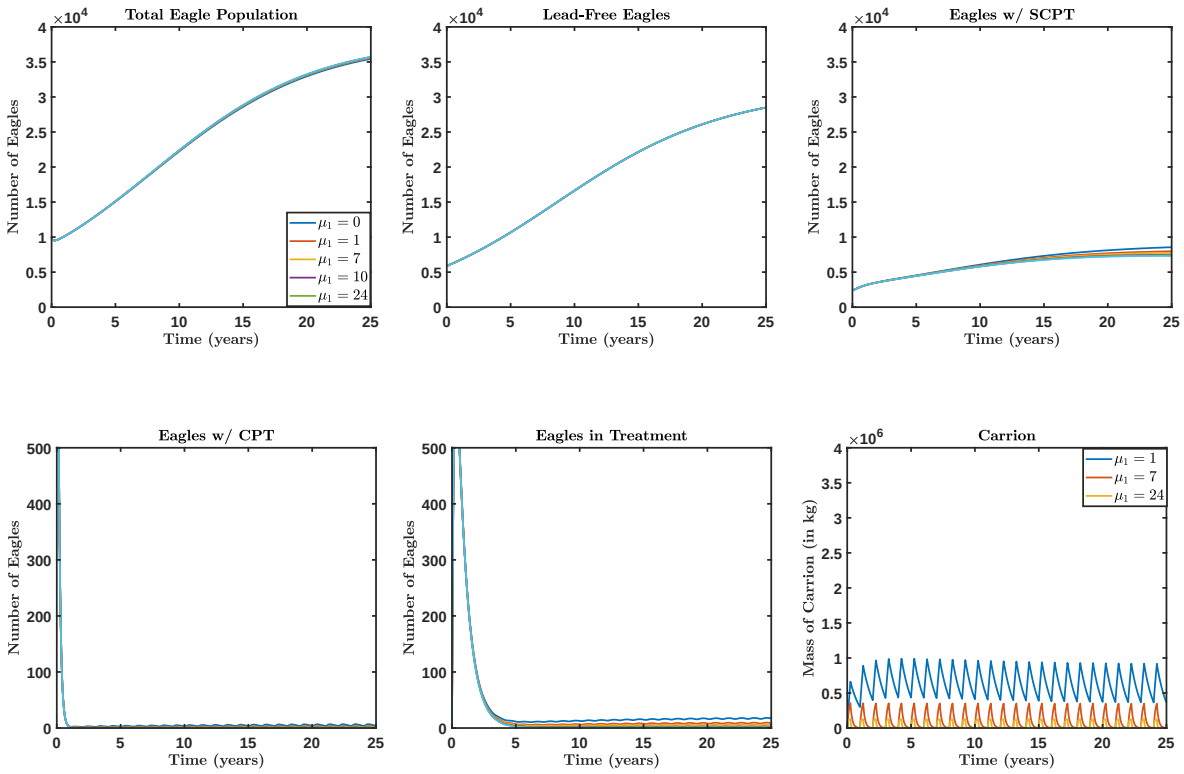

Figure 4: Each panel shows how one of the six state variables (the sixth being the total eagle population, $N = S + L + H + T$) changes for different values of μ_1.

Next we examine the impact of varying the parameter Λ within its largest possible range [0,M], that is, from the case when no carrion is contaminated with lead to the case when all carrion is contaminated with lead.

It is striking to see the difference it makes to reduce the availability of lead-contaminated

carrion. Comparing the extreme cases of going from all-contaminated to none-contaminated, the total eagle population after 25 years would increase from 33,300 to 36,000, an 8.1% increase. Much more extreme is the impact on SCPT eagles: as contaminated carrion increases from none to all, the number of SCPT eagles would increase from 7,300 to 13,700—a huge 88% increase. In the more realistic case of reducing the current 15% contaminated carrion to 0, the impact on the total population after 25 years would still be an increase of 420 eagles (5.8%) accompanied by a decrease of 1,400 eagles with SCPT (16%), as seen in Figure 5.

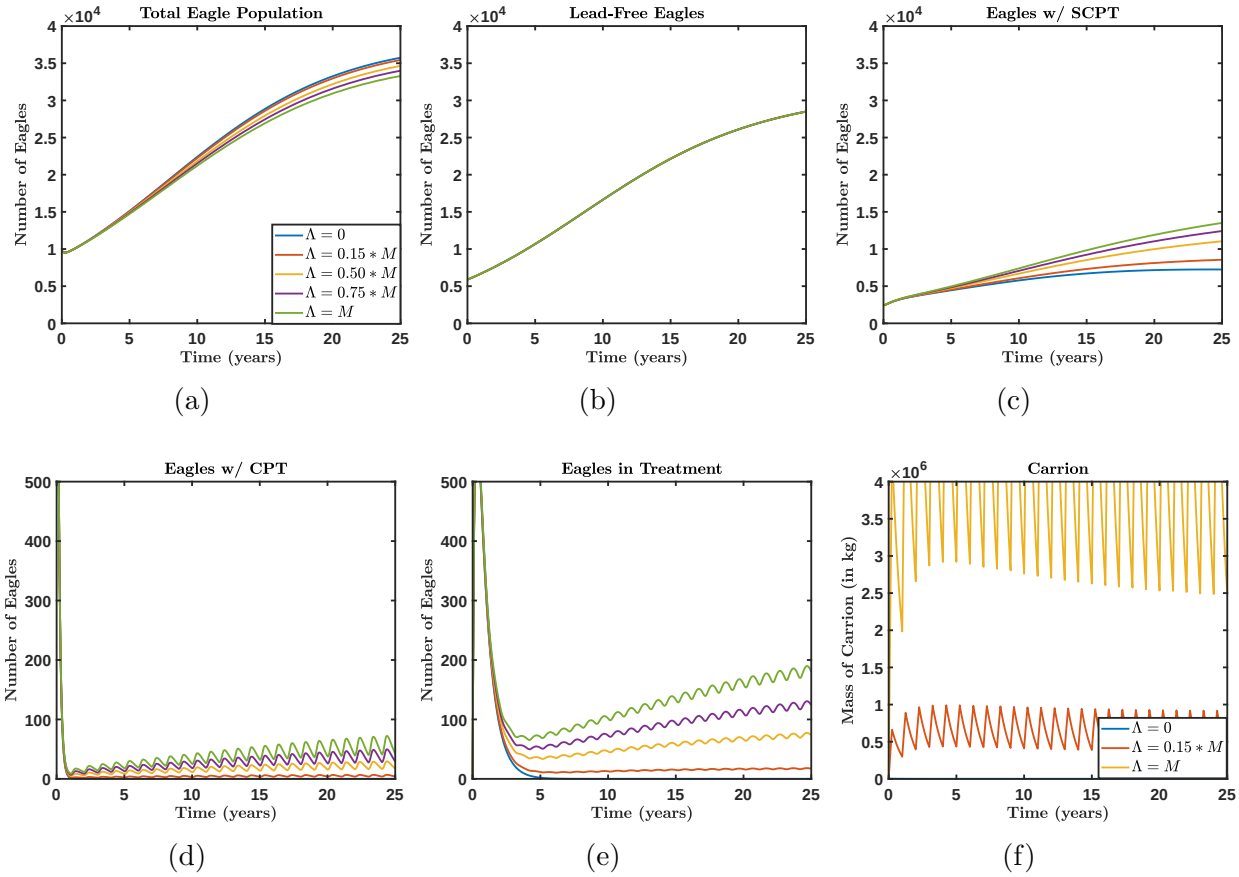

Figure 5: Each panel shows the change in one state variable for different values of Λ.

We finally examine the impact of the parameter η (per capita rate of chelation treatment; its reciprocal $1/\eta$ is the average time it tales for an SCPT eagle to enter treatment) on the population dynamics, because its value is not easily identifiable. We vary it in the interval $[0, 100]$, representing scenarios where SCPT eagles are captured and given treatment after an average of 3.65 days to eternity in the SCPT compartment.

We can see in Figure 6 that η does not have such a large impact on the eagles' population as the other two parameters whose impact we studied in detail. Increasing η from 0 to 100 results, after 25 years, in a 1% increase in their total population, approximately from 35,400 to 35,760. Not surprisingly, the number of eagles under treatment sees the largest percent changes, though their numbers are always less than 30. Looking at more realistic values for η, for example increasing it from 1 to 10 (representing lowering the average time to capture and

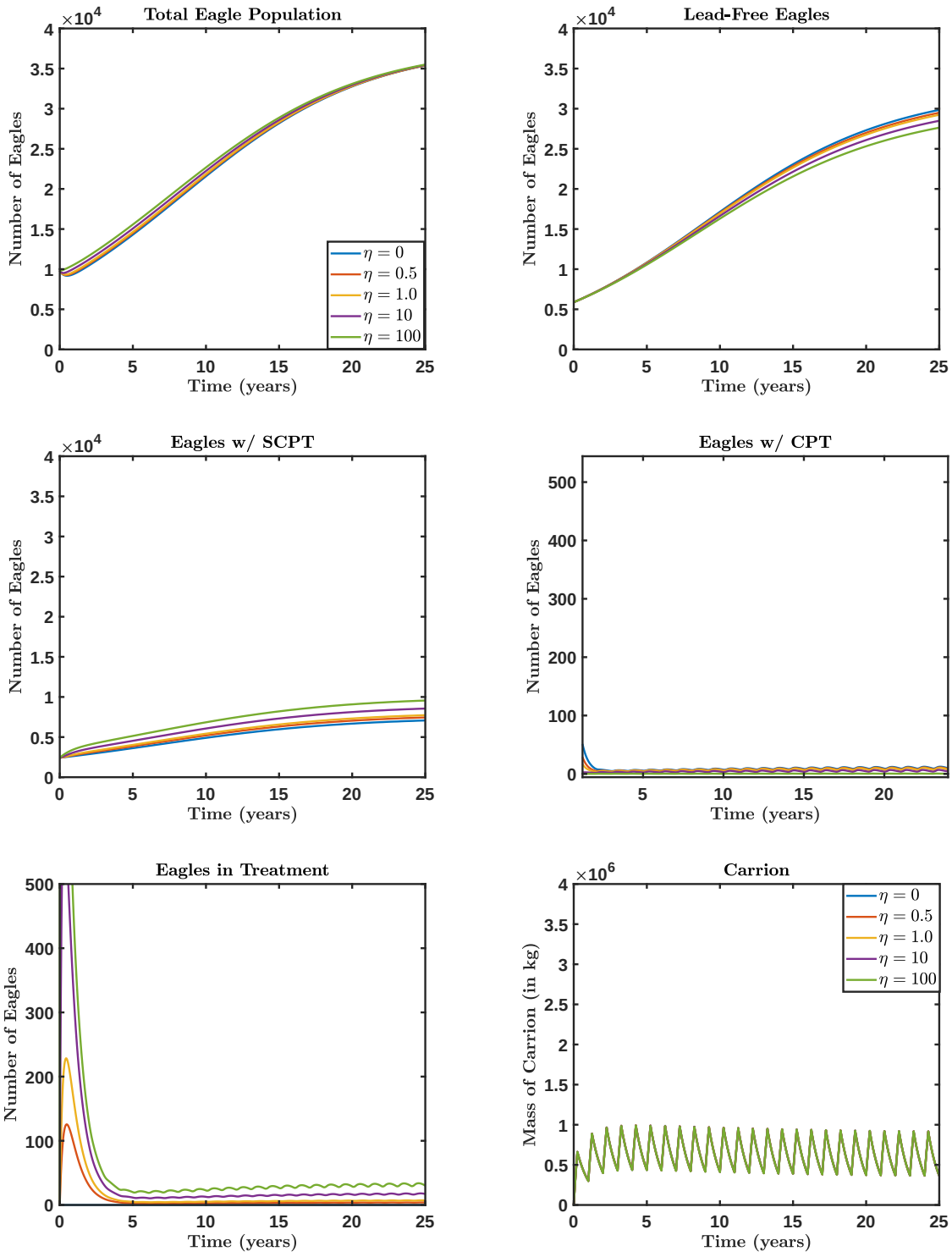

Figure 6: Each panel shows the change in one state variable for different values of η.

treat SCPT eagles from 1 year to about 5 weeks) would only increase the total population of bald eagles by some 30 birds (0.1%).

5 Sensitivity Analysis

Based on the insights from the previous section, we consider the sensitivity indices, or elasticities, of the state variables C, S, L, H, and T with respect to three parameters: the constant rate of the input of lead-contaminated carrion, Λ, the natural unit decay rate of carrion, μ_1, and the per capita treatment rate of eagles with CPT, η, in order to develop a clearer understanding of how much each of these parameters affect each state variable. The sensitivity index ε of a state variable u with respect to a parameter p is defined by

$$\varepsilon_p := \lim_{\delta p \to 0} \frac{\left(\frac{\delta u}{|u|}\right)}{\left(\frac{\delta p}{|p|}\right)} = \frac{|p|}{|u|}\frac{\partial u}{\partial p} = \frac{|p|}{|u|}u_p.$$

The sensitivity index describes the percentage change in the state variable corresponding to a 1% increase in the parameter. We show in Figure 7 the sensitivity indices of all state variables for $0 \leq t \leq 25$.

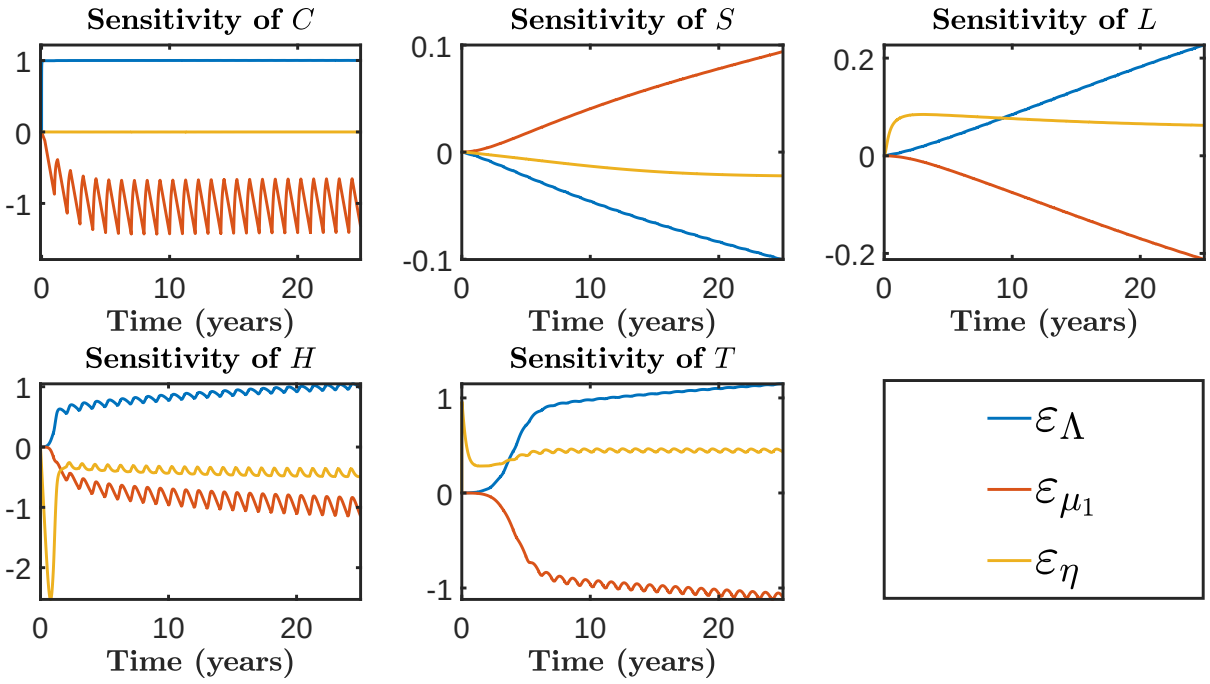

Figure 7: Sensitivity indices of each state variable with respect to Λ, μ_1 and η.

We actually computed the sensitivity indices of the state variables with respect to other parameters too, but they were consistently smaller than those with respect to these three parameters. Therefore, we chose not to plot or report sensitivities with respect to other parameters. We should remark that, in terms of possible real-life impact, these three parameters are the ones that humans can most easily change.

5.1 The Sensitivity of Contaminated Carrion Mass

The sensitivities of C are very different than those for the other compartments. We notice that C is highly sensitive to Λ and μ_1 but not to η. Increasing the input rate of contaminated carrion by 1% will increase the amount of contaminated carrion by about 1%, as intuitively expected. In contrast, a 1% increase in η results in a completely negligible change in C for all time. On the other hand, increasing μ_1 by 1% will make the amount of contaminated carrion decrease by about 1%, which again makes sense intuitively. The oscillations observed in Figure 7 are due to the periodic nature of Λ that is not accompanied by a similar periodic behavior in the other parameters. The actual sensitivities should be read as the average values of the sensitivity index functions. For example, we see that at $t = 25$, the sensitivity index of C with respect to μ_1 is -1.4 (corroborated in the first panel of Figure 8) but the average value of ε_Λ for the state variable C is -1 for $t \geq 5$ (see the first panel of Figure 7).

5.2 The Sensitivity of Eagles' Compartment Sizes

We first examine the sensitivity indices with respect to Λ, the rate at which contaminated carrion enters the environment. Increasing Λ by 1% results in a decrease in S by about 0.1% after 25 years (see Figure 8). This happens because, as eagles in S consume a larger proportion of their scavenged carrion contaminated, they develop SCPT faster. This is also consistent with the sensitivity index for L with respect to Λ: in fact, increasing the input rate of contaminated carrion leads to an increase in the number of eagles with SCPT as more lead-free eagles develop sub-clinical lead toxicity in the same amount of time, while SCPT eagles—that also consume a larger proportion of their scavenged carrion contaminated, thus raising their own lead levels—take longer to develop clinical lead toxicity than lead-free eagles do to develop SCPT. We see that this effect propagates even more through the compartments H and T, which highlights the fact that the entire population is quite sensitive to the input rate of contaminated carrion. To summarize, a 1% increase in Λ results in a 0.1% decrease in S, in a 0.2% increase in L, and 1% increases in H and 1.1% in T (see Figure 8). These peak values after 25 years are reached in an almost linear fashion from 0 at $t = 0$ for both S and L, but much faster (approximately logistically) in the case of H and T (see Figure 7).

Next, we consider sensitivity with respect to μ_1, the natural unit decay rate of carrion. From Figure 8, we see that a 1% increase in μ_1 causes a 0.1% increase in S and decreases in L by 0.2% and in H and T by 1.1%. The explanation is clear: as the contaminated carrion decays faster, the lead-free eagles will have a smaller proportion of the carrion they consume contaminated with lead, thus reducing the development of eagles with SCPT that, at the same time, also have a smaller proportion of the carrion they consume contaminated with lead. Even though eagles with CPT do not consume carrion, their number decreases because of the reduced number of eagles with SCPT developing CPT. Furthermore, decreasing the number of eagles with CPT will reduce the number of eagles that need to be treated for CPT. These sensitivities correspond to $t = 25$. The way they vary from $t = 0$ is very much the same as those with respect to Λ, almost linear from 0 for S and L, and almost logistically for H and T (see Figure 7).

Lastly, an increase in η, the per capita treatment rate of eagles with CPT, by 1% causes decreases in S and H by 0.06% and 0.5%, respectively, and increases in L and T by 0.06%

and 0.4%, respectively. This is consistent with what we expect because treated eagles with CPT never fully recover and return to the SCPT compartment rather than to the lead-free compartment, accounting for both the decrease in S and H and the increase in L. We see in Figure 7 that, except for S—for which ε_η decreases almost linearly from 0 at $t = 0$, the indices ε_η for L, H and T quickly (within 3-4 years) approach values close to those reached at $t = 25$.

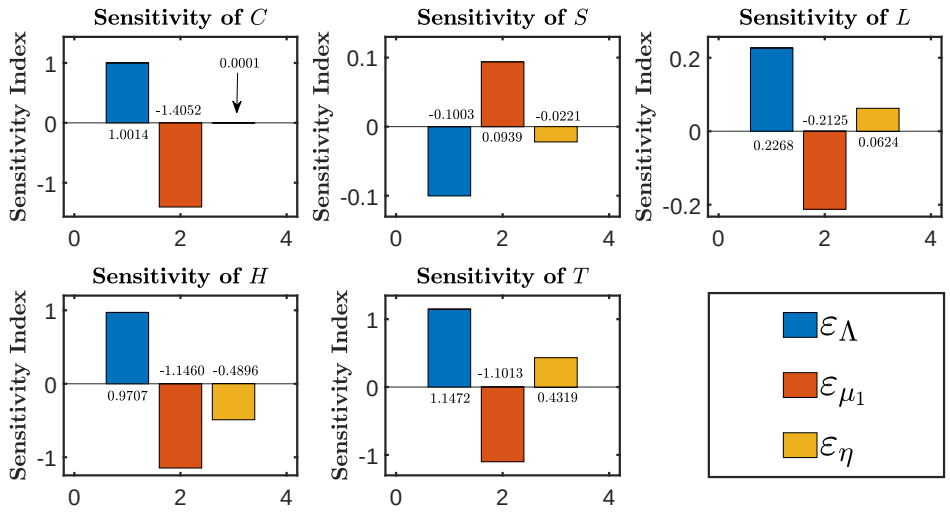

Figure 8: Sensitivity indices of each state variable with respect to Λ, μ_1 and η at $t = 25$.

It is quite useful to see the combined impact of varying Λ and μ_1 on the bald eagles population. We show this in Figure 9, where the height of the surface represents total population of eagles, N.

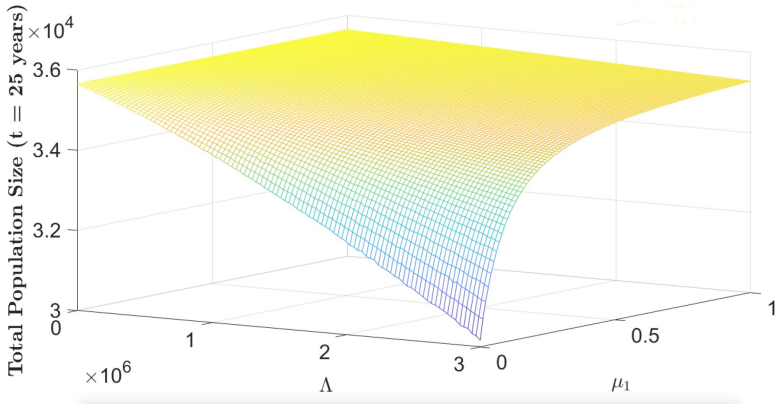

Figure 9: Total population size at $t = 25$ with respect to Λ and μ_1.

Human intervention can increase the value of μ_1 by physically removing contaminated carrion, for example. However, at the current value of Λ, 3,000,000 (represented by the leading edge of the surface), we see that increasing μ_1 from its likely value in the range of 1-20 would have much smaller impact than it would from a low present value, such as 0.1-0.2

say, where the curve on the leading edge is very steep. Those values of μ_1 correspond to a mean permanence of the sources of contamination in the range of 5-10 years, clearly way outside the real-life value for decaying carrion. However, for other ecosystems with different types of toxic substances that do or could stay in the environment for 5-10 years, this surface plot provides a very clear visual representation of the ecological advantage of increasing μ_1 (removal rate of toxic substance) as opposed to decreasing its input rate Λ (note that, for fixed μ_1 in the range 0.1-0.2, the Λ-curves on the surface have much smaller slopes than the μ_1-curves for large values of Λ). This observation is strongly related to the harsh reality that, frequently, financial and political considerations trump ecological ones: even though Λ (rate of toxic input) could be forced down to 0 by law, it is seldom done because that would have a large political cost, while increasing μ_1 (unit removal rate of toxic substance) is usually prohibitively expensive. On the other hand, for the bald eagles population, even without banning leaded ammunition, we see that cutting its use to 1/3 of the present value would have a large positive impact on the total population size and render the value of μ_1 largely irrelevant (the μ_1-curve for $\Lambda = 1$ on the surface is almost horizontal).

6 Discussion

Our model includes logistic growth in the two compartments of lead-free and SCPT eagles as well as vertical transmission of lead toxicity and, therefore, allows for an assessment of its impact on the total bald eagle population's growth. The logistic population growth assumption allowed to fit rather well the 2000, 2007, and 2009 data for the region (see Figure 3). Since the disease we model—lead-toxicity—is not contagious, standard SEIR dynamics for progression through epidemic compartments based on contacts within the population are not applicable. Hence, we used a fifth state variable, mass of contaminated carrion, as a the source and vehicle to move eagles through the stages of the disease. The resulting model is not similar to those for vector-borne or for parasitic diseases because the "vector" in our case is always "infected" and, therefore, only one state variable is needed to model its evolution. Models in the available scientific literature have explored only more general environmental contamination cycles [20, 21].

We explored the demographic and epidemiological consequences of scavenging eagle's consumption of lead-shot-contaminated food-sources, based on three important consequences of chronic exposure: reduction in fertility, reduction in appetite/voracity, and acquisition of clinical lead-toxicity (CPT) that results in death (in the absence of treatment). We explored the sensitivity of the total population size of bald eagles in the Great Lakes region with respect to the three controllable parameters that have the largest impact on the population dynamics: the mass of lead-contaminated carrion (its proportion within the total mass of carrion), Λ, the natural unit decay rate of carrion, μ_1, and the per capita retrieval rate of CPT eagles for chelation treatment, η. We found the largest sensitivity was to the mass of contaminated carrion. This is intuitively expected, because of the long-term physiological damage and the increase in per capita death rate due to lead-toxicity. The impact of Λ of the state variables is shown in Figure 5, panels (a), (c), (d), (e). A similar pattern of sensitivities is observed with respect to the unit decay rate of carrion, μ_1 in Figure 4, panels (a), (c), (d), (e), albeit with smaller impact. In stark contrast, the system has little sensitivity with

respect to η, except for eagles with CPT that are brought into treatment at the per capita rate η and the number of eagles under treatment. However, those eagles are a rather small fraction of the total eagle population and hence large changes in the size of their compartment have little impact on the total population size. We can see that in Figure 6. Figures 4–6 may be misleading in suggesting that the eagle population numbers are more sensitive to η than to μ_1. The reason is that there is no intuitively objective way of assessing sensitivity. Hence, sensitivity indices are used to indicate the percent change in the variable of interest corresponding to a 1% change in the parameter. The value of of those indices with respect to these three parameters are depicted in Figure 8, where their relative importance becomes quite clear..

Our model only considers toxicity-induced eagles deaths as a direct consequence of the lead-toxicity. However, research suggests that the physiological damages caused by chronic lead toxicity also increases the number of deaths due to injury [18, 44]. Although in recent years raptor rehabilitation centers have reported the rising prevalence of lead-toxicity cases, the main cause of non-natural death of eagles is due to other hazards, such as vehicular collision [39]. Typically, these eagles test for elevated serum lead-levels, albeit not high enough to definitively assign the cause of death to lead-poisoning [44]. Several studies conclude that there exists a correlation between deaths due to injuries such as power line and vehicle collisions and the affected flight ability and disorientation of eagles due physiological damage, such as ocular and neurological lesions [9, 11, 31, 39]. This suggests that our analysis may likely be underestimating the damage caused by lead-toxicity in the bald eagle population.

Although there is evidence of lead accumulation in eggshells that suggests the possibility of vertical transmission of lead-toxicity to newborn eaglets [3, 4, 49], this does not imply that all newborn from eagles with SCPT will have SCPT, so that an obvious modification of our model would be the introduction of a parameter representing the probability of vertical transmission of SCPT and separating the offspring of SCPT eagles into the lead-free and SCPT compartments according to that probability.

Concerning the equilibrium x_3^*, we stress that a population of eagles consisting entirely of those with SCPT, represented in Figure 2, panel 3, is likely a mathematical artifact of the model. In the absence of lead-contaminated carrion, there is no evidence to suggest that bald eagles would suffer from chronic lead-toxicity at all.

Although we assume in the model that only eagles with CPT are retrieved and provided with therapy and rehabilitation, in practice eagles with SCPT are also given some treatment, such as fluid administration [9]. To more accurately portray the impact of treatment on the population, future work could incorporate treatment of eagles with SCPT.

7 Conclusion

In conclusion, based on our model, we found that the bald eagle population in the Great Lakes region is not endangered but is clearly suffering from the negative effects of lead-toxicity. The most effective way to reduce this negative effect is by decreasing the input rate of lead-contaminated carrion Λ. In practical terms, a complete removal of that source would be accomplished at a very low cost by replacing the lead-based ammunition used to

hunt with lead-free ammunition (copper-based). The difference in cost between lead and copper ammunition is approximately $0.20 per round. Given that hunters tend to shoot a trial round before the hunt and allowing for two shots per animal hunted, this translates to $0.60 per deer hunted, or a grand total of $540,000 for the 900,000 deer hunted per year. This cost would likely be offset by savings in the capture and treatment of eagles with chronic lead-toxicity but, even without an offset, the predicted 25-year increase in eagle population by 2,700 birds translates to $5,000 per bird—a very small price to pay for the well-being of this natural treasure.

We also found that the system responds much more sharply to changes in the unit decay rate of carrion, μ_1, for larger values of Λ than for smaller ones. This makes an attempt at increasing μ_1 very impractical and costly for the Great Lakes bald eagle ecosystem because it necessitates the physical removal and destruction of contaminated carrion. On the other hand, for other ecological systems involving contaminants with a very slow decay rate, their removal (clean-up) may be by far the most efficient measure to reduce the level of contamination in a population affected by it, as clearly suggested by the interplay between the input of contaminant into the environment and its unit decay rate depicted in Figure 9.

8 Acknowledgments

The authors would like to thank the Offices of the Provost and of the Dean of The College of Liberal Arts and Sciences of Arizona State University for funding this research.

References

[1] Environmental Protection Agency. Facts and Figures about the Great Lakes. https://www.epa.gov/greatlakes/facts-and-figures-about-great-lakes. Accessed: 2020-07-22.

[2] Bryan Bedrosian, Derek Craighead, and Ross Crandall. Lead exposure in bald eagles from big game hunting, the continental implications and successful mitigation efforts. *PloS one*, 7(12):e51978, 2012.

[3] Jason E. Bruggeman, William T. Route, Patrick T. Redig, and Rebecca L. Key. Patterns and trends in lead (Pb) concentrations in bald eagle (Haliaeetus leucocephalus) nestlings from the western Great Lakes region. *Ecotoxicology*, 27(5):605–618, jul 2018.

[4] Joanna Burger. Heavy metals in avian eggshells: Another excretion method. *Journal of Toxicology and Environmental Health*, 41(2):207–220, 1994.

[5] National Eagle Center. Eagle diet & feeding. https://www.nationaleaglecenter.org/eagle-diet-feeding/, 2020.

[6] Luis Cruz-Martinez, Patrick T Redig, and John Deen. Lead from spent ammunition: a source of exposure and poisoning in bald eagles. *Human-Wildlife Interactions*, 6(1):94–104, 2012.

[7] James Estes, Kevin Crooks, and Robert D. Holt. Predators, ecological role of. In Simon A. Levin, editor, *Encyclopedia of Biodiversity*, volume 4, pages 857–878. San Diego: Academic Press, 2001.

[8] James A. Estes, John Terborgh, Justin S. Brashares, Mary E. Power, Joel Berger, William J. Bond, Stephen R. Carpenter, Timothy E. Essington, Robert D. Holt, Jeremy B. C. Jackson, Robert J. Marquis, Lauri Oksanen, Tarja Oksanen, Robert T. Paine, Ellen K. Pikitch, William J. Ripple, Stuart A. Sandin, Marten Scheffer, Thomas W. Schoener, Jonathan B. Shurin, Anthony R. E. Sinclair, Michael E. Soulé, Risto Virtanen, and David A. Wardle. Trophic downgrading of planet earth. *Science*, 333(6040):301–306, 2011.

[9] Jesse A. Fallon, Patrick Redig, Tricia A. Miller, Michael Lanzone, and Todd Katzner. Guidelines for evaluation and treatment of lead poisoning of wild raptors. *Wildlife Society Bulletin*, 41(2):205–211, jun 2017.

[10] Center for Biological Diversity. Bald eagle population exceeds 11,000 pairs in 2007: Long-term trend for each state available for first time. https://www.biologicaldiversity.org/species/birds/bald_eagle/report/index.html.

[11] J. Christian Franson and Robin E. Russell. Lead and eagles: demographic and pathological characteristics of poisoning, and exposure levels associated with other causes of mortality. *Ecotoxicology*, 23(9):1722–1731, oct 2014.

[12] Jennifer Freed and Alan Yarbrough. Health consultation: The Potential for Ingestion Exposure to Lead Fragments in Venison in Wisconsin. Technical report, U.S. Department of Health & Human Services, Atlanta, GA, 2008.

[13] Laura Gangoso, Pedro Álvarez-Lloret, Alejandro A.B. Rodríguez-Navarro, Rafael Mateo, Fernando Hiraldo, and José Antonio Donázar. Long-term effects of lead poisoning on bone mineralization in vultures exposed to ammunition sources. *Environmental Pollution*, 157(2):569–574, feb 2009.

[14] Kathrin Ganz, Lukas Jenni, Milena M. Madry, Thomas Kraemer, Hannes Jenny, and David Jenny. Acute and Chronic Lead Exposure in Four Avian Scavenger Species in Switzerland. *Archives of Environmental Contamination and Toxicology*, 75(4):566–575, nov 2018.

[15] José M. Gil-Sánchez, Saray Molleda, José A. Sánchez-Zapata, Jesús Bautista, Isabel Navas, Raquel Godinho, Antonio J. García-Fernández, and Marcos Moleón. From sport hunting to breeding success: Patterns of lead ammunition ingestion and its effects on an endangered raptor. *Science of the Total Environment*, 613-614:483–491, feb 2018.

[16] C E Gill and K M Langelier. British columbia. acute lead poisoning in a bald eagle secondary to bullet ingestion. *The Canadian veterinary journal = La revue veterinaire canadienne*, 35(5):303, 1994.

[17] Nancy H. Golden, Sarah E. Warner, and Michael J. Coffey. A review and assessment of spent lead ammunition and its exposure and effects to scavenging birds in the United States. In *Reviews of Environmental Contamination and Toxicology*, volume 237, pages 123–191. Springer New York LLC, Falls Church, VA, 2016.

[18] Hunt W. Grainger. Implications of Sublethal Lead Exposure in Avian Scavengers. *Journal of Raptor Research*, 46(4):389–393, 2012.

[19] Susan M. Haig, Jesse D'Elia, Collin Eagles-Smith, Jeanne M. Fair, Jennifer Gervais, Garth Herring, James W. Rivers, and John H. Schulz. The persistent problem of lead poisoning in birds from ammunition and fishing tackle. *The Condor*, 116(3):408–428, aug 2014.

[20] T G Hallam, C E Clark, and G S Jordan. Effects of Toxicants on Populations: A Qualitative Approach II. First Order Kinetics. Technical report, University of Tennessee, Department of Mathematics, 1983.

[21] T.G. Hallam, C.E. Clark, and R.R. Lassiter. Effects of toxicant on population: A Qualitative Approach I. Equilibrium environmental exposure. *Ecological Modelling*, 18(3):291–304, 1983.

[22] The Mathworks, Inc. MATLAB R2020a (Version 9.8) [Computer Software]. https://www.mathworks.com/. Natick, Massachusetts, USA.

[23] Wolfram Research, Inc. Mathematica, Version 12.1 [Computer Software]. https://www.wolfram.com/mathematica. Champaign, IL, 2020.

[24] Christopher S. Jennelle, Michael D. Samuel, Cherrie A. Nolden, and Elizabeth A. Berkley. Deer carcass decomposition and potential scavenger exposure to chronic wasting disease. *Journal of Wildlife Management*, 73(5):655–662, 2009.

[25] Global Great Lakes. Laurentian Great Lakes. http://www.globalgreatlakes.org/lgl/. Accessed: 2020-07-22.

[26] Ronald A. Lindblom, Letitia M. Reichart, Brett A. Mandernack, Matthew Solensky, Casey W. Schoenebeck, and Patrick T. Redig. INFLUENCE OF SNOWFALL ON BLOOD LEAD LEVELS OF FREE-FLYING BALD EAGLES (HALIAEETUS LEUCOCEPHALUS) IN THE UPPER MISSISSIPPI RIVER VALLEY. *Journal of Wildlife Diseases*, 53(4):816 – 823, 2017.

[27] Martin Lodenius and Tapio Solonen. The use of feathers of birds of prey as indicators of metal pollution. *Ecotoxicology*, 22(9):1319–1334, nov 2013.

[28] Ryan Magana, Austin Dixon, Cala Hakseth, Carly Lapin, Laura Jaskiewicz, Skyler Vold, Joseph Henry, Jake Koebernik, Jim Woodford, Tyler Boudry, Dean Edlin, Rich Staffen, Sharon Fandel, and Ryan Clemo. Wisconsin Bald Eagle and Osprey Nest Surveys 2019. Technical report, Wisconsin Department of Natural Resources, 2019.

[29] Leah K. Manning, Arno Wünschmann, Anibal G. Armién, Michelle Willette, Kathleen MacAulay, Jeff B. Bender, John P. Buchweitz, and Patrick Redig. Lead Intoxication in Free-Ranging Bald Eagles (Haliaeetus leucocephalus). *Veterinary Pathology*, 56(2):289–299, mar 2019.

[30] Maple Inc. Maple (2019) [Computer Software]. https://www.maplesoft.com/. Waterloo, Ontario.

[31] Kay Neumann. Bald Eagle Lead Poisoning in Winter. In R. T. Watson, M. Fuller, M. Pokras, and W. G. Hunt (Eds.). Ingestion of Lead from Spent Ammunition: Implications for Wildlife and Humans. 2009.

[32] Charles M Nixon, Lonnie P Hansen, Paul A Brewer, James E Chelsvig, Terry L Esker, Dwayne Etter, Joseph B Sullivan, Robert G Koerkenmeier, and Philip C Mankin. Survival of white-tailed deer in intensively farmed areas of illinois. *Canadian Journal of Zoology*, 79(4):581–588, 2001.

[33] University of California Santa Barbara. Apex predators. http://scienceline.ucsb.edu/getkey.php?key=4532. Accessed: 2020-07-23.

[34] Missouri Department of Conservation. Deer Harvest Summary 2012–2013. https://huntfish.mdc.mo.gov/hunting-trapping/species/deer/deer-harvest-reports/deer-harvest-summaries/deer-harvest-summary-2012.

[35] Indiana Department of Natural Resources. *Bald Eagle*. 2020.

[36] Deborah J. Pain, Rafael Mateo, and Rhys E. Green. Effects of lead from ammunition on birds and other wildlife: A review and update. *Ambio*, 48(9):935–953, sep 2019.

[37] Patrick T. Redig, Lori Arent, Hugo Lopes, and Luis Cruz. Rehabilitation. In David M. Bird, Keith Bildstein, David R. Barber, and Andrea Zimmerman, editors, *Raptor Research and Management Techniques*, chapter 23, pages 411–422. Hancock House, Blaine, WA, 2 edition, 2007.

[38] Patrick T. Redig, Lori Arent, Hugo Lopes, and Luis Cruz. Toxicology. In David M. Bird, Keith Bildstein, David R. Barber, and Andrea Zimmerman, editors, *Raptor Research and Management Techniques*, chapter 23, pages 411–422. Hancock House, Blaine, WA, 2 edition, 2007.

[39] Robin E. Russell and J. Christian Franson. Causes of mortality in eagles submitted to the National Wildlife Health Center 1975-2013. *Wildlife Society Bulletin*, 38(4):697–704, dec 2014.

[40] U.S. Fish & Wildlife Service. Great Lakes Basin Ecosystem Team. https://www.fws.gov/midwest/fisheries/Library/fact-ecoteam.pdf. Accessed: 2020-07-22.

[41] U.S. Fish & Wildlife Service. Bald eagle breeding pairs 1990 to 2006. https://www.fws.gov/midwest/eagle/NestingData/nos_state_tbl.html, May 2020.

[42] U.S. Fish & Wildlife Service. Nest chronology of bald eagles in the midwest. https://www.fws.gov/midwest/eagle/Nhistory/NestChron.html#nesting, May 2020.

[43] Stephanie Shepherd. Bald Eagle (Halieetus leucocephalus) status in Iowa, 2019. Technical report, Iowa Department of Natural Resources, Boone, IA, 2019.

[44] Kendall L. Simon, David A. Best, James G. Sikarskie, H. Tyler Pittman, William W. Bowerman, Thomas M. Cooley, and Scott Stolz. Sources of Mortality in Bald Eagles in Michigan, 1986–2017. *Journal of Wildlife Management*, 84(3):553–561, apr 2020.

[45] Erik Stauber, Nickol Finch, Patricia A. Talcott, and John M. Gay. Lead Poisoning of Bald (Haliaeetus leucocephalus) and Golden (Aquila chrysaetos) Eagles in the US Inland Pacific Northwest Region—An 18-year Retrospective Study: 1991–2008. *Journal of Avian Medicine and Surgery*, 24(4):279–287, dec 2010.

[46] Sean M. Strom, Julie A. Langenberg, Nancy K. Businga, and Jasmine K. Batten. Lead Exposure in Wisconsin Birds. Technical report, Wisconsin Department of Natural Resources, Madison, WI.

[47] Courtney Turrin and Bryan D. Watts. Intraspecific intrusion at bald eagle nests. *Ardea*, 102(1):71–78, 2014.

[48] U.S. Fish & Wildlife Service. Bald and Golden Eagles: Population demographics and estimation of sustainable take in the United States, 2016 update. Technical report, 2016.

[49] Núria Vallverdú-Coll, Ana López-Antia, Monica Martinez-Haro, Manuel E. Ortiz-Santaliestra, and Rafael Mateo. Altered immune response in mallard ducklings exposed to lead through maternal transfer in the wild. *Environmental Pollution*, 205:350–356, jun 2015.

[50] Sarah E. Warner, Edward E. Britton, Drew N. Becker, and Michael J. Coffey. Bald eagle lead exposure in the Upper Midwest. *Journal of Fish and Wildlife Management*, 5(2):208–216, dec 2014.

[51] Michael A. Watt, Andrew S. Norton, Tim R. Van Deelen, Karl J. Martin, Shelli A. Dubay, Jared F. Duquette, Camille H. Warbington, and Robert E. Rolley. Wisconsin Deer Research Studies, Annual Report 2011-2012. Technical report, Wisconsin Department of Natural Resouces, University of Wisconsin-Madison, Madison, WI, 2012.

[52] Rebecca F. Wisch. Detailed discussion of the bald and golden ealge protection act. *Michigan State University College of Law*, 2002.

[53] Wisconsin Department of Natural Resources. 2019 Wisconsin HUnting and Trapping Seasons. Technical report, Wisconsin Department of Natural Resources, 2019.

[54] Taylor Yaw, Kay Neumann, Linette Bernard, Jodeane Cancilla, Terese Evans, Adam Martin-Schwarze, and Bianca Zaffarano. Lead poisoning in bald eagles admitted to wildlife rehabilitation facilities in Iowa, 2004-2014. *Journal of Fish and Wildlife Management*, 8(2):465–473, dec 2017.